
A Differential Game Theoretic Neural Optimizer for Training Residual Networks

Guan-Horng Liu, Tianrong Chen, and Evangelos A. Theodorou
Autonomous Control and Decision Systems Laboratory
Georgia Institute of Technology, Atlanta, GA 30332
{ghliu, tianrong.chen, evangelos.theodorou}@gatech.edu

Abstract

Connections between Deep Neural Networks (DNNs) training and optimal control theory has attracted considerable attention as a principled tool of algorithmic design. Differential Dynamic Programming (DDP) neural optimizer [1] is a recently proposed method along this line. Despite its empirical success, the applicability has been limited to feedforward networks and whether such a trajectory-optimization inspired framework can be extended to modern architectures remains unclear. In this work, we derive a generalized DDP optimizer that accepts both residual connections and convolution layers. The resulting optimal control representation admits a game theoretic perspective, in which training residual networks can be interpreted as cooperative trajectory optimization on state-augmented dynamical systems. This Game Theoretic DDP (GT-DDP) optimizer enjoys the same theoretic connection in previous work, yet generates a much complex update rule that better leverages available information during network propagation. Evaluation on image classification datasets (e.g. MNIST and CIFAR100) shows an improvement in training convergence and variance reduction over existing methods. Our approach highlights the benefit gained from architecture-aware optimization.

1 Introduction

Attempts from different disciplines to provide a fundamental understanding of deep learning have advanced rapidly in recent years. Among those, interpretation of DNNs as discrete-time nonlinear dynamical systems, by viewing each layer as a distinct time step, has received tremendous focus as it enables rich analysis ranging from numerical equations [2], mean-field theory [3], to physics [4, 5, 6]. For instance, interpretation of residual networks as a discretization of ordinary differential equations (ODEs) [7] provides theoretical reasoning on its optimization landscape [8]. It also inspires new architecture that inherits numerical stability [9, 10, 11] and differential limit [12, 13].

Development of practical optimization methods, however, remains relatively limited. This is primarily because classical approach to optimize dynamical systems relies on the optimal control theory, which typically considers systems with neither the dimensionality nor parameterization as high as DNNs. Such a difficulty limits its application, despite showing promising convergence and robustness in trajectory optimization [14], to mostly theoretical interpretation of DNNs training [15, 16]. The algorithmic progress has been restricted to either specific network class (e.g. discrete weight [17]) or training procedure (e.g. hyper-parameter adaptation [18] or computational acceleration [19, 20]), until the recently proposed Differential Dynamic Programming (DDP) optimizer [1].

DDP is a second-order optimizer built upon a formal connection between trajectory optimization and training feedforward networks, and from such it suggests existing training algorithms can be lifted to embrace the dynamic programming principle, resulting in superior parameter updates with layer-wise feedback policies. However, DDP is an *architecture-dependent* optimizer, in that the

feedback policies need to be derived on a per architecture basis. This raises questions of its flexibility and scalability to training modern architectures such as residual networks [21], since the existing formulation scales exponentially with the batch size (see Fig. 1).

In this work, we present a game-theoretic extension to the DDP optimizer (GT-DDP) which arises naturally from the optimal control representation of residual networks. GT-DDP treats each layer as a decision maker in a multi-stage coalition game connected through network propagation. This leads to much complex feedback policies as information is allowed to be exchanged between layers. Despite the increasing computation, we leverage efficient approximations which enable GT-DDP to run on a faster wall-clock yet with less memory (see Fig. 1). On the theoretical side, we extend previous analysis for feedforward networks to *arbitrary* architecture (Proposition 4), and derive game-theoretic integration for existing second-order optimizers (Theorem 3 and Corollary 7). GT-DDP shows an overall improvement on image classification dataset.

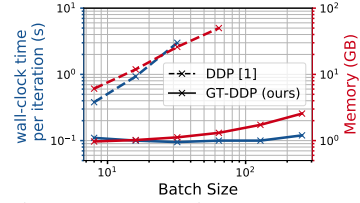


Figure 1: Comparison on MNIST.

There has been a rising interest in game-theoretic analysis since the landmark Generative Adversarial Network [22]. By framing networks into a two-player competing game, prevalent efforts have been spent on studying its convergence dynamics [23] and effective optimizers to find stable saddle points [24, 25]. Notably, our layer-as-player formulation has appeared in Balduzzi [26] to study the signal communication implied in the Back-propagation, yet without any practical algorithm being made. On the other hand, the cooperative game framework has been used to discover neuron contribution in representation learning and network pruning [27, 28], which are of independent interest for this work.

The paper is organized as follows. We first review the connection between optimal control and DNNs training in Sec. 2. Extending such framework to residual networks is then given in Sec. 3, with GT-DDP demonstrated in Sec. 4. We provide empirical results and discussion in Sec. 5 and 6.

2 Preliminaries

2.1 Optimal Control Formulation of Training DNNs

Classical optimal control problem (OCP) in discrete time considers the following programming:

$$\min_{\bar{\mathbf{u}}} J(\bar{\mathbf{u}}; \mathbf{x}_0) := \left[\phi(\mathbf{x}_T) + \sum_{t=0}^{T-1} \ell_t(\mathbf{x}_t, \mathbf{u}_t) \right] \quad \text{s.t. } \mathbf{x}_{t+1} = f_t(\mathbf{x}_t, \mathbf{u}_t), \quad (1)$$

where $\mathbf{x}_t \in \mathbb{R}^{n_t}$ and $\mathbf{u}_t \in \mathbb{R}^{m_t}$ represent the state and control at each time step $t \in \{0, \dots, T\}$. f_t , ℓ_t and ϕ respectively denote the dynamics, intermediate cost and terminal cost. The control trajectory is denoted as $\bar{\mathbf{u}} \triangleq \{\mathbf{u}_t\}_{t=0}^{T-1}$. Eq. (1) can be interpreted as the training objective of DNNs by treating \mathbf{x}_t and \mathbf{u}_t as the vectorized activation map (\mathbf{x}_0 and \mathbf{x}_T being input image and prediction vector) and weight at each layer t . f_t stands as the compositional module propagating the activation vector, e.g. an affine transformation followed by an element-wise activation in a feedforward network. ℓ_t and ϕ denote the per-layer regularization (e.g. weight decay) and terminal loss (e.g. cross-entropy).

Following these notations, the gradient descent (GD) update at iteration k can be written as $\bar{\mathbf{u}}^{(k+1)} = \bar{\mathbf{u}}^{(k)} + \delta \bar{\mathbf{u}}^* = \bar{\mathbf{u}}^{(k)} - \eta \nabla_{\bar{\mathbf{u}}} J$, where η is the learning rate. We can further break down the update for the full network to each layer, i.e. $\delta \bar{\mathbf{u}} \triangleq \{\delta \mathbf{u}_t\}_{t=0}^{T-1}$, computed backward by

$$\delta \mathbf{u}_t^* = \arg \min_{\delta \mathbf{u}_t \in \mathbb{R}^{m_t}} \left\{ J_t + \nabla_{\mathbf{u}_t} J_t^\top \delta \mathbf{u}_t + \frac{1}{2} \delta \mathbf{u}_t^\top \left(\frac{1}{\eta} \mathbf{I}_t \right) \delta \mathbf{u}_t \right\}, \quad (2)$$

$$\text{where } J_t(\mathbf{x}_t, \mathbf{u}_t) \triangleq \ell_t(\mathbf{u}_t) + J_{t+1}(f_t(\mathbf{x}_t, \mathbf{u}_t), \mathbf{u}_{t+1}), \quad J_T(\mathbf{x}_T) \triangleq \phi(\mathbf{x}_T) \quad (3)$$

is the per-stage objective¹ at layer t . It can be readily verified that $\nabla_{\mathbf{x}_t} J_t$ gives the exact Back-propagation dynamics. Eq. (2) follows the standard optimization interpretation in which GD minimizes the second-order Taylor expansion of J_t with its Hessian $\nabla_{\mathbf{u}_t}^2 J_t$ replaced by $\frac{1}{\eta} \mathbf{I}_t$, i.e. spherical

Notation: t will always be denoted the time step of dynamics, or equivalently the layer’s index. Given a time-dependent function $\mathcal{F}_t(\mathbf{x}_t, \mathbf{u}_t) : \mathbb{X} \times \mathbb{U} \mapsto \mathbb{R}$, we will denote and sometimes abbreviate it Jacobian, Hessian, and mixed partial derivative respectively as $\nabla_{\mathbf{x}_t} \mathcal{F}_t \equiv \mathcal{F}_{\mathbf{x}_t}^t$, $\nabla_{\mathbf{x}_t}^2 \mathcal{F}_t \equiv \mathcal{F}_{\mathbf{x}_t \mathbf{x}_t}^t$, and $\nabla_{\mathbf{x}_t} \nabla_{\mathbf{u}_t} \mathcal{F}_t \equiv \mathcal{F}_{\mathbf{x}_t \mathbf{u}_t}^t$.

¹ We drop \mathbf{x}_t in all $\ell_t(\cdot)$ hereafter as the layer-wise regularization typically involves network weight alone.

Algorithm 1 DDP Neural Optimizer (at iteration k)

- 1: **Input:** forward pass $\{\mathbf{x}_t\}_{t=0}^T$ with weights $\bar{\mathbf{u}}^{(k)}$
 - 2: Set $V_{\mathbf{x}}^T = \nabla_{\mathbf{x}}\phi$ and $V_{\mathbf{x}\mathbf{x}}^T = \nabla_{\mathbf{x}\mathbf{x}}^2\phi$
 - 3: **for** $t = T - 1$ **to** 0 **do**
 - 4: Compute derivatives of Q_t with $V_{\mathbf{x}}^{t+1}, V_{\mathbf{x}\mathbf{x}}^{t+1}$
 - 5: Compute $\mathbf{k}_t, \mathbf{K}_t, V_{\mathbf{x}}^t$ and $V_{\mathbf{x}\mathbf{x}}^t$
 - 6: **end for**
 - 7: Set $\hat{\mathbf{x}}_0 = \mathbf{x}_0$
 - 8: **for** $t = 0$ **to** $T - 1$ **do**
 - 9: $\hat{\mathbf{u}}_t = \mathbf{u}_t^{(k)} + \mathbf{k}_t + \mathbf{K}_t\delta\mathbf{x}_t, \quad (\delta\mathbf{x}_t = \hat{\mathbf{x}}_t - \mathbf{x}_t)$
 - 10: $\hat{\mathbf{x}}_{t+1} = f_t(\hat{\mathbf{x}}_t, \hat{\mathbf{u}}_t)$
 - 11: **end for**
 - 12: $\bar{\mathbf{u}}^{(k+1)} \leftarrow \{\hat{\mathbf{u}}_t\}_{t=0}^{T-1}$
-

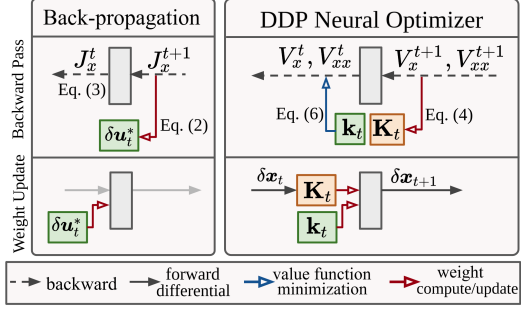


Figure 2: Comparison of computational graphs in feedforward networks.

curvature. In a similar vein, adaptive first-order methods, such as RMSprop and Adam, approximate $\nabla_{\mathbf{u}_t}^2 J_t$ by diagonal matrices with the leading entries adapting to the second-moment statistics in each coordinate. Second-order optimizers like KFAC [29, 30] and EKfAC [31] compute much complex non-diagonal curvature matrices with Gauss-Newton approximation, i.e. $\nabla_{\mathbf{u}_t}^2 J_t \approx J_{\mathbf{u}_t}^T J_{\mathbf{u}_t}$.

2.2 Differential Dynamic Programming Neural Optimizer

Differential Dynamic Programming (DDP) is a second-order trajectory optimization algorithm that solves the same programming in Eq. (1). Instead of searching updates from \mathbb{R}^{m_t} , at each decision stage DDP aims at finding a locally-optimal *feedback* policy, i.e. $\delta\mathbf{u}_t(\delta\mathbf{x}_t) \in \Gamma_{\delta\mathbf{x}_t}$, where $\Gamma_{\delta\mathbf{x}_t} = \{\mathbf{b}_t + \mathbf{A}_t\delta\mathbf{x}_t : \mathbf{b}_t \in \mathbb{R}^{m_t}, \mathbf{A}_t \in \mathbb{R}^{m_t \times n_t}\}$ denotes all possible affine mappings from the state differential $\delta\mathbf{x}_t$. The resulting per-stage updates can also be computed backward:

$$\delta\mathbf{u}_t^*(\delta\mathbf{x}_t) = \arg \min_{\delta\mathbf{u}_t \in \Gamma_{\delta\mathbf{x}_t}} \left\{ Q_t + \frac{1}{2} \begin{bmatrix} \mathbf{1} \\ \delta\mathbf{x}_t \\ \delta\mathbf{u}_t \end{bmatrix}^\top \begin{bmatrix} \mathbf{0} & Q_{\mathbf{x}}^t & Q_{\mathbf{u}}^t \\ Q_{\mathbf{x}\mathbf{x}}^t & Q_{\mathbf{x}\mathbf{u}}^t & Q_{\mathbf{u}\mathbf{x}}^t \\ Q_{\mathbf{u}\mathbf{x}}^t & Q_{\mathbf{u}\mathbf{x}}^t & Q_{\mathbf{u}\mathbf{u}}^t \end{bmatrix} \begin{bmatrix} \mathbf{1} \\ \delta\mathbf{x}_t \\ \delta\mathbf{u}_t \end{bmatrix} \right\}, \quad (4)$$

$$\text{where } V_t(\mathbf{x}_t) \triangleq \min_{\mathbf{u}_t \in \Gamma_{\mathbf{x}_t}} \underbrace{\ell_t(\mathbf{u}_t) + V_{t+1}(f_t(\mathbf{x}_t, \mathbf{u}_t))}_{Q_t(\mathbf{x}_t, \mathbf{u}_t) \equiv Q_t}, \quad V_T(\mathbf{x}_T) \triangleq \phi(\mathbf{x}_T) \quad (5)$$

is the *value* function that summarizes the objective value when all the afterward stages, i.e. $Q_{s \geq t}$, are minimized. Hereafter we will denote the quadratic expansion in Eq. (4) as $\delta Q_t(\delta\mathbf{x}_t, \delta\mathbf{u}_t)$. Q_t will be referred to the *Bellman objective*, as Eq. (5) is well-known as the *Bellman equation* [32].

The analytic solution to Eq. (4) is given by $\delta\mathbf{u}_t^*(\delta\mathbf{x}_t) = \mathbf{k}_t + \mathbf{K}_t\delta\mathbf{x}_t$, where $\mathbf{k}_t \triangleq -(Q_{\mathbf{u}\mathbf{u}}^t)^{-1}Q_{\mathbf{u}}^t$ and $\mathbf{K}_t \triangleq -(Q_{\mathbf{u}\mathbf{u}}^t)^{-1}Q_{\mathbf{u}\mathbf{x}}^t$ are the locally optimal open and feedback gains. From the chain rule, evaluating the derivatives of Q_t in Eq. (4) requires one to compute $V_{\mathbf{x}}^{t+1}$ and $V_{\mathbf{x}\mathbf{x}}^{t+1}$. These quantities can be obtained by simply substituting $\delta\mathbf{u}_t^*(\delta\mathbf{x}_t)$ to Eq. (5) at each stage:

$$\begin{aligned} V_{\mathbf{x}}^t &= \nabla_{\mathbf{x}_t} \{Q_t + \delta Q_t(\delta\mathbf{x}_t, \delta\mathbf{u}_t^*(\delta\mathbf{x}_t))\} = Q_{\mathbf{x}}^t + Q_{\mathbf{x}\mathbf{u}}^t \mathbf{k}_t, \\ V_{\mathbf{x}\mathbf{x}}^t &= \nabla_{\mathbf{x}_t}^2 \{Q_t + \delta Q_t(\delta\mathbf{x}_t, \delta\mathbf{u}_t^*(\delta\mathbf{x}_t))\} = Q_{\mathbf{x}\mathbf{x}}^t + Q_{\mathbf{x}\mathbf{u}}^t \mathbf{K}_t. \end{aligned} \quad (6)$$

It is obvious that Eq. (4, 5) resemble Eq. (2, 3) in several ways. Both classes of optimizer perform quadratic approximation of the stage-wise objective, except DDP also expands the objective wrt $\delta\mathbf{x}_t$, which requires computing the mixed partial derivatives $Q_{\mathbf{u}\mathbf{x}}^t$. The theoretical connection between these two approaches for feedforward networks has been made formally in Liu et al. [1].

Proposition 1 ([1]). *When $Q_{\mathbf{u}\mathbf{x}}^t = \mathbf{0}$ at all stages, the first-order derivative of the value function collapses to the Back-propagation gradient in feedforward networks, i.e. $V_{\mathbf{x}}^t = J_{\mathbf{x}}^t$. In this case, DDP computes the same update in stage-wise Newton²: $\delta\mathbf{u}_t^*(\delta\mathbf{x}_t) = -(J_{\mathbf{u}\mathbf{u}}^t)^{-1}J_{\mathbf{u}}^t$. If we further assume $Q_{\mathbf{u}\mathbf{u}}^t = \frac{1}{\eta}\mathbf{I}_t$, then DDP degenerates to the Back-propagation with gradient descent.*

Proposition 1 suggests that by setting $Q_{\mathbf{u}\mathbf{x}}^t = \mathbf{0}$ and choosing a proper $Q_{\mathbf{u}\mathbf{u}}^t$, we can recover existing optimizers from DDP. Meanwhile, existing methods can be extended to accept DDP framework by computing $Q_{\mathbf{u}\mathbf{x}}^t$. The resulting layer-wise feedback policies generate weight update with additional forward pass (lines 7-11 in Alg. 1), in which the state differential is computed. We summarize the backward pass and weight update procedure of the DDP optimizer in Alg. 1 and Fig. 2.

² Stage-wise Newton preconditioned the gradient by the block-wise inverse Hessian at each layer.

3 Optimal Control Representation for Residual Networks

In this section, we extend the Bellman optimization framework to networks consist of residual paths. Despite that in the Back-propagation this simply involves merging additional gradient flow from the shortcut, its optimal control representation is much complex when second-order information and Bellman minimization are involved. We leave the complete derivation in the Appendix A.

3.1 Residual Connection as State-Augmented Dynamics

Consider the residual network in Fig. 3a. Let us denote \mathbf{x}_r as the residual state shortcutting from the layer t_s to t_f , so that the output is merged by $\mathbf{x}_{t_f+1} = \mathbf{x}_r + f_{t_f}(\mathbf{x}_{t_f}, \mathbf{u}_{t_f})$. The Bellman equation along the residual path is given by

$$V_{t_s}(\mathbf{x}_{t_s}) = \min_{\mathbf{u}_{t \in [t_s, t_f]}} \ell_{t_s}(\mathbf{u}_{t_s}) + \dots + \ell_{t_f}(\mathbf{u}_{t_f}) + V_{t_f+1}(\mathbf{x}_r + (f_{t_f} \circ \dots \circ f_{t_s})(\mathbf{x}_{t_s})), \quad (7)$$

which can be decomposed into the following minimization and solve recursively from t_f :

$$V_t(\mathbf{x}_r, \mathbf{x}_t) = \min_{\mathbf{u}_t} Q_t(\mathbf{x}_r, \mathbf{x}_t, \mathbf{u}_t) := \begin{cases} \ell_t(\mathbf{u}_t) + V_{t+1}(\mathbf{x}_r + f_t(\mathbf{x}_t, \mathbf{u}_t)), & t = t_f \\ \ell_t(\mathbf{u}_t) + V_{t+1}(\mathbf{x}_r, f_t(\mathbf{x}_t, \mathbf{u}_t)), & t \in (t_s, t_f) \end{cases} \quad (8a)$$

$$V_{t_s}(\mathbf{x}_{t_s}) = \min_{\mathbf{u}_{t_s}} Q_{t_s}(\mathbf{x}_{t_s}, \mathbf{u}_{t_s}) := \ell_{t_s}(\mathbf{u}_{t_s}) + V_{t_s+1}(\mathbf{x}_{t_s}, f_{t_s}(\mathbf{x}_{t_s}, \mathbf{u}_{t_s})) \quad (8b)$$

Eq. (8) suggests the value functions of layers parallel to the shortcut depend not only on its own state \mathbf{x}_t but also the residual \mathbf{x}_r . This is better explained from the game theoretic viewpoint. As \mathbf{x}_r affects the payoff obtained during $t \in [t_s, t_f]$ through the addition at $t_f + 1$, it shall contribute to decisions made at these stages. Notice that we can rewrite the propagation rule as state-augmented dynamics $\hat{f}_t(\mathbf{x}_r, \mathbf{x}_t, \mathbf{u}_t)$. Dynamics of such forms resemble *time-delayed* systems [33], $f(\mathbf{x}_{t-i}, \dots, \mathbf{x}_t, \mathbf{u}_t)$. Instead of a constant moving window, here we consider a fixed time stamp anchored at t_s .

The new DDP update can be solved similar to Eq. (4), except the Bellman objective should be expended additionally wrt to $\delta \mathbf{x}_r$. The optimal feedback law thus depends on the differential of both states:

$$\delta \mathbf{u}_t^*(\delta \mathbf{x}_t, \delta \mathbf{x}_r) = \mathbf{k}_t + \mathbf{K}_t \delta \mathbf{x}_t + \mathbf{G}_t \delta \mathbf{x}_r, \quad \text{where } \mathbf{G}_t \triangleq -(Q_{\mathbf{u}\mathbf{u}}^t)^{-1} f_{\mathbf{u}}^T V_{\mathbf{x}\mathbf{x}_r}^{t+1} \quad (9)$$

is the optimal residual feedback gain. \mathbf{k}_t and \mathbf{K}_t are the same open and feedback gains computed in the absence of shortcut. Thus, the new update rule has an additional feedback from the channel of residual state (cf. Fig. 3b). The term $V_{\mathbf{x}\mathbf{x}_r}^{t+1}$ denotes the mixed partial derivatives of $V_{t+1}(\mathbf{x}_r, \mathbf{x}_{t+1})$, quantifying how these two states should be correlated mathematically. It can be computed, together with the residual value Hessian $V_{\mathbf{x}_r, \mathbf{x}_r}^{t+1}$, through backward recursions similar to Eq. (6),

$$V_{\mathbf{x}\mathbf{x}_r}^t = f_{\mathbf{x}}^T V_{\mathbf{x}\mathbf{x}_r}^{t+1} - \mathbf{K}_t^T Q_{\mathbf{u}\mathbf{u}}^t \mathbf{G}_t, \quad V_{\mathbf{x}_r, \mathbf{x}_r}^t = V_{\mathbf{x}_r, \mathbf{x}_r}^{t+1} - \mathbf{G}_t^T Q_{\mathbf{u}\mathbf{u}}^t \mathbf{G}_t, \quad (10)$$

with the terminal conditions given by $V_{\mathbf{x}\mathbf{x}_r}^{t_f+1} = V_{\mathbf{x}_r, \mathbf{x}_r}^{t_f+1} = V_{\mathbf{x}\mathbf{x}}^{t_f+1}$.

It is natural to ask how the optimal control representation differs between residual and feedforward networks. This is summarized in the following proposition.

Proposition 2. *When networks contain shortcut from t_s to t_f , the derivatives of the value function at stage t_s , denoted $\tilde{V}_{\mathbf{x}}^{t_s}$ and $\tilde{V}_{\mathbf{x}\mathbf{x}}^{t_s}$, relate to the ones in feedforward networks, denoted $V_{\mathbf{x}}^{t_s}$ and $V_{\mathbf{x}\mathbf{x}}^{t_s}$, by*

$$\tilde{V}_{\mathbf{x}}^{t_s} = V_{\mathbf{x}}^{t_s} + V_{\mathbf{x}}^{t_f+1} - \sum_{t \in [t_s, t_f]} \mathbf{G}_t^T Q_{\mathbf{u}\mathbf{u}}^t \mathbf{k}_t, \quad (11)$$

$$\tilde{V}_{\mathbf{x}\mathbf{x}}^{t_s} = V_{\mathbf{x}\mathbf{x}}^{t_s} + V_{\mathbf{x}\mathbf{x}}^{t_f+1} - \sum_{t \in [t_s, t_f]} \mathbf{G}_t^T Q_{\mathbf{u}\mathbf{u}}^t \mathbf{G}_t + V_{\mathbf{x}\mathbf{x}_r}^{t_s} + V_{\mathbf{x}\mathbf{x}_r}^{t_s T} \quad (12)$$

There are several interesting implications from Proposition 2. First, recall that in the Back-propagation, the gradient at t_s is obtained by simply merging the one from the shortcut, i.e. $\tilde{J}_{\mathbf{x}}^{t_s} = J_{\mathbf{x}}^{t_s} + J_{\mathbf{x}}^{t_f+1}$. In the Bellman framework, $\tilde{V}_{\mathbf{x}}^{t_s}$ is modified in a similar manner, yet with an additional summation coming from the Bellman minimization along the shortcut. Interpretation for $\tilde{V}_{\mathbf{x}\mathbf{x}}^{t_s}$ follows the same road map, except the mixed partial derivative $V_{\mathbf{x}\mathbf{x}_r}^{t_s}$ also contributes to the Hessian of the value function at t_s . We highlight these traits which distinguish our work from both standard Back-propagation and previous work [1].

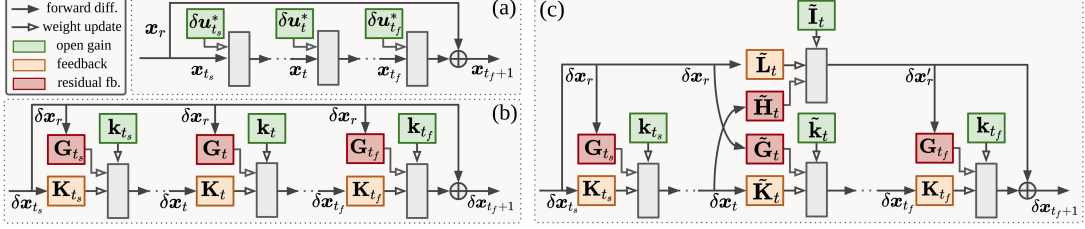


Figure 3: Terminology and weight update graph for (a) standard Back-propagation and (b)(c) GT-DDP optimizer with identity and arbitrary shortcut mapping.

3.2 Cooperative Trajectory Optimization with Non-identity Shortcut Mapping

In some cases, the dimension of feature map between t_s and t_f may be mismatched; thus the residual path will contain a non-identity shortcut mapping [34]. For CNNs this is typically achieved by down-sampling x_r with an 1×1 convolution. Hereafter we will denote this non-identity mapping as $x'_r = h_t(x_r, v_t)$, where v_t is the vectorized weight. The new Bellman equation, consider for instance when we add the mapping to the middle of residual path, i.e. $t \in (t_s, t_f)$ in Eq. (8b), becomes

$$V_t(x_r, x_t) = \min_{\mathbf{u}_t, \mathbf{v}_t} \underbrace{\ell(\mathbf{u}_t) + \ell(\mathbf{v}_t) + V_{t+1}(h_t(x_r, \mathbf{v}_t), f_t(x_t, \mathbf{u}_t))}_{\triangleq Q_t(x_r, x_t, \mathbf{u}_t, \mathbf{v}_t)}. \quad (13)$$

Minimizing $Q_t(x_r, x_t, \mathbf{u}_t, \mathbf{v}_t)$ simultaneously wrt \mathbf{u}_t and \mathbf{v}_t resembles the formulation in a complete Cooperative Game (CG) [35]. In its common setup, two players observe the same state and decide their policies to maximize a *cooperative* payoff. The game is *complete* in that all information is known and shared in prior; thus can be leveraged to make better decisions. Application of DDP to solving CG has been studied previously in robotics for robust trajectory optimization [36].

Before solving Eq. (13), it will be useful to first revisit cases when each policy can be solved independently, i.e. when $Q_t(x_r, x_t, \mathbf{u}_t, \mathbf{v}_t) = Q_t(x_t, \mathbf{u}_t) + Q_t(x_r, \mathbf{v}_t)$. In this case, we know $\mathbf{k}_t, \mathbf{K}_t$ is the solution to $\arg \min_{\mathbf{u}_t} Q_t(x_t, \mathbf{u}_t)$. Let us further denote $\mathbf{I}_t + \mathbf{L}_t \delta x_r = \arg \min_{\mathbf{v}_t} Q_t(x_r, \mathbf{v}_t)$, where $\mathbf{I}_t \triangleq -(Q_{vv}^t)^{-1} Q_v^t$ and $\mathbf{L}_t \triangleq -(Q_{vv}^t)^{-1} Q_{v\mathbf{x}_r}^t$. Now, solving Eq. (13) by quadratically expanding $Q_t(x_r, x_t, \mathbf{u}_t, \mathbf{v}_t)$ wrt all variables will arrive at the following form³:

$$\delta \mathbf{u}_t^*(\delta x_t, \delta x_r) = \tilde{\mathbf{k}}_t + \tilde{\mathbf{K}}_t \delta x_t + \tilde{\mathbf{G}}_t \delta x_r \quad (14)$$

$$= -\tilde{Q}_{uu}^{-1} \left(\underbrace{Q_{uu}^t + Q_{uv}^t \mathbf{I}_t}_{\tilde{Q}_{uu}^t} + \underbrace{(Q_{ux}^t - Q_{uv}^t Q_{vv}^{-1} Q_{vx}^t)}_{\tilde{Q}_{ux}^t} \delta x_t + \underbrace{(Q_{ux_r}^t + Q_{uv}^t \mathbf{L}_t)}_{\tilde{Q}_{ux_r}^t} \delta x_r \right),$$

$$\delta \mathbf{v}_t^*(\delta x_t, \delta x_r) = \tilde{\mathbf{I}}_t + \tilde{\mathbf{L}}_t \delta x_r + \tilde{\mathbf{H}}_t \delta x_t \quad (15)$$

$$= -\tilde{Q}_{vv}^{-1} \left(\underbrace{Q_v^t + Q_{vu}^t \mathbf{k}_t}_{\tilde{Q}_{vv}^t} + \underbrace{(Q_{v\mathbf{x}_r}^t - Q_{vu}^t Q_{uu}^{-1} Q_{u\mathbf{x}_r}^t)}_{\tilde{Q}_{v\mathbf{x}_r}^t} \delta x_r + \underbrace{(Q_{v\mathbf{x}}^t + Q_{vu}^t \mathbf{K}_t)}_{\tilde{Q}_{v\mathbf{x}}^t} \delta x_t \right),$$

where $\tilde{Q}_{uu}^t \triangleq Q_{uu}^t - Q_{uv}^t Q_{vv}^{-1} Q_{vu}^t$ and $\tilde{Q}_{vv}^t \triangleq Q_{vv}^t - Q_{vu}^t Q_{uu}^{-1} Q_{uv}^t$ result from the block-matrices inversion with the Schur complement. The update rules provided in Eq. (14, 15) are much complex and do not admit forms of superposition as in Eq. (9). To make some intuitions, compare for instance the open gain $\mathbf{k}_t \triangleq -Q_{uu}^{-1} Q_u^t$ with its cooperative variant $\tilde{\mathbf{k}}_t \triangleq -\tilde{Q}_{uu}^{-1} (Q_u^t + Q_{uv}^t \mathbf{I}_t)$. The latter adjusts the policy by knowing the companion's update rule \mathbf{I}_t , and information between two players' actions communicates through Q_{uv} and Q_{vu} . Similar interpretation can be drawn for the feedback gains \mathbf{K}_t and $\tilde{\mathbf{K}}_t$, as Q_{vu} allows information to flow from Q_{ux} through Q_{vx} , and etc.

Fig. 3c illustrates how these feedback policies generate the weight update. \mathbf{k}_t and \mathbf{K}_t are applied in the same manner as in feedforward networks (c.f. Fig. 2). Layers parallel to the skip connection receive additional residual feedback from \mathbf{G}_t . At the decision stage when the non-identity shortcut mapping is involved, policies will be modified to their cooperative form, i.e. $\tilde{\mathbf{k}}_t, \tilde{\mathbf{K}}_t, \tilde{\mathbf{G}}_t, \tilde{\mathbf{I}}_t, \tilde{\mathbf{L}}_t, \tilde{\mathbf{H}}_t$. Notice that the residual policies $\mathbf{G}_{s \leq t}$ and $\mathbf{G}_{s > t}$ now take *different* state differential (δx_r and $\delta x'_r$, resp.). This implies the GT-DDP solution to residual networks is not unique, as placing $h_t(x_r, v_t)$ at different location along the shortcut will result in different value of weight update. Despite seemingly unintuitive, from the game theoretic perspective it implies one would prefer $\delta x'_r$ to δx_r whenever the former is available, since states closer to the decision stage reveal more information.

³ We omit the superscript t of $Q_{uu}^{-1}, Q_{vv}^{-1}, \tilde{Q}_{uu}^{-1}, \tilde{Q}_{vv}^{-1}$ sometimes for notational simplicity but stress that Q is always time (i.e. layer) dependent in this work.

Table 1: Relation between existing first (e.g. RMSprop) and second-order (e.g. EKFAC) algorithms under GT-DDP framework⁴

	Q_{uu}, Q_{vv}	Q_{uv}, Q_{vu}	nonzero $Q_{ux},$ Q_{vx}, Q_{ux_r}, Q_{vx}
RMSprop	$\frac{1}{\eta} \text{diag}(J_u \odot J_u + \epsilon)$	$\mathbf{0}$	\times
GT-DDP-RMSprop	$\frac{1}{\eta} \text{diag}(Q_u \odot Q_u + \epsilon)$	$\mathbf{0}$	\checkmark
EKFAC	$\mathbb{E}[\mathbf{x}\mathbf{x}^\top] \otimes \mathbb{E}[J_h J_h^\top]$	$\mathbf{0}$	\times
GT-DDP-EKFAC	$\mathbb{E}[\mathbf{x}\mathbf{x}^\top] \otimes \mathbb{E}[V_h V_h^\top]$	Theorem 3	\checkmark

4 Game Theoretic DDP Neural Optimizer

In this section we discuss efficient computation of the update rules proposed in the previous section to training residual networks. As the algorithm generalizes the DDP framework [1] to new architectures under game-theoretic perspective, we name it the Game Theoretic DDP neural optimizer (GT-DDP). Detailed derivation and proof in this section are left in the Appendix B.

4.1 Curvature Approximation

Computation of the GT-DDP solution involves extensive evaluation of the derivatives of Q_t wrt different variables. Since f_t is highly over-parametrized in each network layer, second-order derivatives wrt the weight parameter, e.g. Q_{uu}^t, Q_{vv}^t , are particularly expensive to compute, let alone their inversions. Thus, approximation must be made for these matrices.

Following the curvature interpretation in Sec 2.1, one can simply substitute these expensive Hessians with the ones considered in existing methods. For instance, replacing Q_{uu}^t with an identity (or diagonal) matrix resembles the (adaptive) first-order update rule. Note that this first-order approximation implicitly implies both Q_{uv}^t and Q_{vu}^t to vanish, since by construction first-order methods omit the covariances among different weight coordinate.

As for second-order approximation, in this work we consider the popular Kronecker factorization used in EKFAC [31]. Let $f_t \equiv \sigma(\mathbf{W}_t \mathbf{x}_t + \mathbf{b}_t)$ be the generic dynamics where σ is the activation function, and denote $\mathbf{h}_t \equiv \mathbf{W}_t \mathbf{x}_t + \mathbf{b}_t$ as the pre-activation vector. EKFAC factorizes $Q_{uu}^t \approx \mathbb{E}[\mathbf{x}_t \mathbf{x}_t^\top] \otimes \mathbb{E}[\mathbf{g}_t \mathbf{g}_t^\top]$, where \otimes is the Kronecker operator and $\mathbf{g}_t := J_{\mathbf{h}}^t$ is the first-order derivative of the per-stage objective wrt the pre-activation vector⁵. The expectation is taken wrt the batch sample. Factorizing GT-DDP with Kronecker operation requires one to derive the Kronecker representations for the cooperative matrices appeared in CG, which are given below.

Theorem 3 (Kronecker factorization in Cooperative Game). *Suppose Q_{uu} and Q_{vv} are factorized respectively by $Q_{uu} \approx A_{uu} \otimes B_{uu}$ and $Q_{vv} \approx A_{vv} \otimes B_{vv}$, where*

$$A_{uu} \triangleq \mathbb{E}[\mathbf{x}_u \mathbf{x}_u^\top], \quad B_{uu} \triangleq \mathbb{E}[\mathbf{g}_u \mathbf{g}_u^\top], \quad A_{vv} \triangleq \mathbb{E}[\mathbf{x}_v \mathbf{x}_v^\top], \quad B_{vv} \triangleq \mathbb{E}[\mathbf{g}_v \mathbf{g}_v^\top]$$

are the Kronecker block matrices for layers $f(\mathbf{x}_u, \mathbf{u})$ and $h(\mathbf{x}_v, \mathbf{v})$. Further, let $A_{uv} \triangleq \mathbb{E}[\mathbf{x}_u \mathbf{x}_v^\top]$ and $B_{uv} \triangleq \mathbb{E}[\mathbf{g}_u \mathbf{g}_v^\top]$, then the unique Kronecker factorizations for the matrices in CG are given by

$$\tilde{Q}_{uu}^{-1} \approx \tilde{A}_{uu}^{-1} \otimes \tilde{B}_{uu}^{-1} = (A_{uu} - A_{uv} A_{vv}^{-1} A_{uv}^\top)^{-1} \otimes (B_{uu} - B_{uv} B_{vv}^{-1} B_{uv}^\top)^{-1} \quad (16)$$

$$\tilde{Q}_{vv}^{-1} \approx \tilde{A}_{vv}^{-1} \otimes \tilde{B}_{vv}^{-1} = (A_{vv} - A_{uv}^\top A_{uu}^{-1} A_{uv})^{-1} \otimes (B_{vv} - B_{uv}^\top B_{uu}^{-1} B_{uv})^{-1}, \quad (17)$$

and $Q_{uv} = Q_{vu}^\top \approx -A_{uv} \otimes B_{uv}$. The CG update, take $\tilde{\mathbf{k}}_t$ for example, can be computed by

$$\tilde{\mathbf{k}}_t = -\text{vec}(\tilde{B}_{uu}^{-1} (Q_u + B_{uv} B_{vv}^{-1} Q_v A_{vv}^\top A_{uv}^\top) \tilde{A}_{uu}^{-\top}). \quad (18)$$

Hereafter we will refer these approximations respectively to *GT-DDP-RMSprop*, *GT-DDP-EKFAC*, and etc. The algorithmic relation between existing methods and their DDP integration is summarized in Table 1, with the theoretical connection given by the following proposition.

Proposition 4. *The update rules derived from stage-wise minimization of the Bellman equation degenerate to the method it uses to approximate the weight Hessian, i.e. Q_{uu}, Q_{vv} , when the Bellman objective Q_t at all stages satisfies (i) all mixed partial derivatives between parameter and activation, e.g. Q_{ux}, Q_{ux_r} , vanish, and (ii) parameters between distinct layers are uncorrelated.*

⁴ \odot denotes element-wise multiplication. \mathbf{h} is the pre-activation vector defined in Sec. 4.

⁵ For GT-DDP-EKFAC, we have $\mathbf{g}_t := V_{\mathbf{h}}^t$. We left further introduction and derivation in Appendix B.1.

Note that Proposition 4 extends Proposition 1 to *arbitrary* architectures beyond feedforward and residual networks, so long as its layer-wise Bellman objective is properly defined.

4.2 Practical Implementation

Block-diagonal Value Hessian: Extending the Bellman optimization framework to accept mini-batch samples $\{\mathbf{x}_0^{(i)}\}_{i=0}^B$ has been made in previous work [1] by augmenting the state space to $\mathbf{x}'_t = [\dots, \mathbf{x}_t^{(i)}, \dots]^\top$. However, such a formulation can cause memory explosion when \mathbf{x}_t is lifted to 3D feature map in convolutional layers, let alone the augmented value function considered in GT-DDP (cf Eq. (8)). In this work, we propose to approximate the batch-augmented value Hessian $V_{\mathbf{x}'\mathbf{x}'}$ as block-diagonal. The approximation is made from an empirical observation (see Fig. 4) that $V_{\mathbf{x}'\mathbf{x}'}$ contains only nontrivial values along the diagonal blocks, even when networks contain Batch Normalization (BN) layers. This suggests one can reduce the memory consumption by approximating the batch-augmented value Hessian as block-diagonal and only carry batch matrices, $\{V_{\mathbf{x}^{(i)}\mathbf{x}^{(i)}}^t\}_{i=0}^B$, along the backward computation.

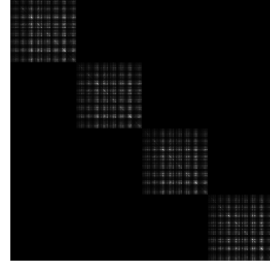


Figure 4: Example of $V_{\mathbf{x}'\mathbf{x}'}$ for batch size $B = 4$ in DIGITS dataset. Higher (whiter) values concentrate along the diagonal blocks $V_{\mathbf{x}^{(i)}\mathbf{x}^{(i)}}^t$.

Gauss-Newton (GN) Approximation at the Terminal Hessian: Next, we impose Gauss-Newton approximation to the Hessian at the prediction layer. Surprisingly, this will lead to a nontrivial factorization in the Bellman optimization framework. For dynamics represented by feedforward networks, we have the following proposition.

Proposition 5 (Outer-product factorization in DDP). *Consider the following form of OCP:*

$$\min_{\mathbf{u}} \left[\phi(\mathbf{x}_T) + \sum_{t=0}^{T-1} \ell_t(\mathbf{u}_t) \right] \quad \text{s.t. } \mathbf{x}_{t+1} = f_t(\mathbf{x}_t, \mathbf{u}_t). \quad (19)$$

If the Hessian of the terminal loss can be expressed by an outer product of vectors, i.e. $\nabla^2 \phi(\mathbf{x}_T) \approx \mathbf{z}_x^T \otimes \mathbf{z}_x^T$ for some vector \mathbf{z}_x^T (e.g. $\mathbf{z}_x^T = \nabla \phi$ for GN approximation), then we have the factorization:

$$\forall t, \quad Q_{\mathbf{u}\mathbf{u}}^t = \mathbf{q}_u^t \otimes \mathbf{q}_u^t, \quad Q_{\mathbf{x}\mathbf{x}}^t = \mathbf{q}_x^t \otimes \mathbf{q}_x^t, \quad V_{\mathbf{x}\mathbf{x}}^t = \mathbf{z}_x^t \otimes \mathbf{z}_x^t, \quad (20)$$

where \mathbf{q}_u^t , \mathbf{q}_x^t , and \mathbf{z}_x^t are outer-product vectors which can be computed backward:

$$\mathbf{q}_u^t = f_u^T \mathbf{z}_x^{t+1}, \quad \mathbf{q}_x^t = f_x^T \mathbf{z}_x^{t+1}, \quad \mathbf{z}_x^t = \sqrt{1 + \mathbf{q}_u^T (Q_{\mathbf{u}\mathbf{u}}^t)^{-1} \mathbf{q}_u} \mathbf{q}_x^t. \quad (21)$$

In other words, the outer-product factorization at the final stage can be backward propagated to all proceeding layers. Thus, *state-dependent* second-order matrices can be represented as outer products of vectors. We note that the low-rank structure at the prediction layer has been observed when classification loss (e.g. cross-entropy) is used [37, 38]. Prop. 5 can be extended to residual networks:

Proposition 6 (Outer-product factorization in GT-DDP). *The residual value Hessians considered in Eq. (10), when the same outer-product factorization is imposed at the terminal stage, take the form*

$$V_{\mathbf{x}\mathbf{x}_r}^t = \mathbf{z}_x^t \otimes \mathbf{z}_{x_r}^t \quad \text{and} \quad V_{\mathbf{x}_r\mathbf{x}_r}^t = \mathbf{z}_{x_r}^t \otimes \mathbf{z}_{x_r}^t, \quad \text{where } \mathbf{z}_{x_r}^t = \sqrt{1 + \mathbf{q}_u^T (Q_{\mathbf{u}\mathbf{u}}^t)^{-1} \mathbf{q}_u} \mathbf{z}_{x_r}^{t+1} \quad (22)$$

and $(\mathbf{q}_u^t, \mathbf{q}_x^t, \mathbf{z}_x^t)$ are given by Eq. (21). When the non-identity shortcut mapping, i.e. $h_t(\mathbf{x}_r, \mathbf{v}_t)$ in Eq. (13), is presented, the cooperative forms of \mathbf{z}_x^t and $\mathbf{z}_{x_r}^t$, denoted $\tilde{\mathbf{z}}_x^t$ and $\tilde{\mathbf{z}}_{x_r}^t$, are given by

$$\tilde{\mathbf{z}}_x^t = \sqrt{1 + \mathbf{q}_u^T Q_{\mathbf{u}\mathbf{u}}^{-1} \mathbf{q}_u + \mathbf{q}_v^T Q_{\mathbf{v}\mathbf{v}}^{-1} \mathbf{q}_v} \mathbf{q}_x^t, \quad \tilde{\mathbf{z}}_{x_r}^t = \sqrt{1 + \mathbf{q}_u^T Q_{\mathbf{u}\mathbf{u}}^{-1} \mathbf{q}_u + \mathbf{q}_v^T Q_{\mathbf{v}\mathbf{v}}^{-1} \mathbf{q}_v} \mathbf{q}_{x_r}^t, \quad (23)$$

where $\mathbf{q}_{x_r}^t = h_{x_r}^T \mathbf{z}_{x_r}^{t+1}$, and $\mathbf{q}_v^t = h_v^T \mathbf{z}_{x_r}^{t+1}$.

The outer-product factorization, together with the block-diagonal approximation, reduces the computational dependency by dropping the memory by 2/3 and the runtime by 1/5 compared with previous work [1], as shown in Fig. 1. As such, we adopt both approximation in all experiments.

Jacobian of Layers Dynamics: Finally, computing the derivatives of the Bellman objective involve evaluating the Jacobian associated with each layer, e.g. $Q_{\mathbf{x}}^t = f_x^T V_{\mathbf{x}}^{t+1}$ and $Q_{\mathbf{u}}^t = f_u^T V_{\mathbf{x}}^{t+1}$. These computations can be done efficiently for both fully-connected (FC) and convolution (Conv) layers:

$$f_x^T V_{\mathbf{x}}^{t+1} = \begin{cases} \mathbf{W}_t^T V_{\mathbf{h}}^t \\ \omega_t^T \hat{*} V_{\mathbf{h}}^t \end{cases}, \quad f_x^T V_{\mathbf{x}}^{t+1} = \begin{cases} \mathbf{x}_t \otimes V_{\mathbf{h}}^t \\ \mathbf{x}_t \hat{*} V_{\mathbf{h}}^t \end{cases}, \quad \text{where } f_x^t = \sigma_t(\mathbf{h}_t), \quad \mathbf{h}_t \triangleq \begin{cases} \mathbf{W}_t \mathbf{x}_t + \mathbf{b}_t \\ \omega_t * \mathbf{x}_t \end{cases}$$

respectively denote the pre-activation of FC and Conv layers. $*$ and $\hat{*}$ denote the convolution and deconvolution (transposed convolution) operator [39, 40].

5 Evaluation on Classification Data Set

Table 2: Performance comparison on train loss and validation accuracy (over 6 random seeds). (+) and (-) respectively denote improvement and degradation over non-GT-DDP baselines.

Data Set		SGD	RMSProp	Adam	EKFAC	GT-DDP -SGD	GT-DDP -RMSProp	GT-DDP -Adam	GT-DDP -EKFAC
Training	DIGITS	0.0053	0.0247	0.0182	0.0514	0.0050 (+)	0.0124 (+)	0.0081 (+)	0.0514 (+)
	MNIST	0.0250	0.0284	0.0330	0.0290	0.0240 (+)	0.0282 (+)	0.0312 (+)	0.0291 (-)
	SVHN	0.2755	0.2670	0.2544	0.2049	0.2692 (+)	0.2637 (+)	0.2517 (+)	0.2047 (+)
	CIFAR-10	0.0296	0.0107	0.0127	0.0922	0.0284 (+)	0.0069 (+)	0.0096 (+)	0.0907 (+)
	CIFAR-100	0.0075	0.0058	0.0055	0.0120	0.0075 (-)	0.0058 (+)	0.0054 (+)	0.0125 (-)
Validation (%)	DIGITS	96.09	95.61	95.81	95.31	96.10 (+)	95.92 (+)	95.84 (+)	95.55 (+)
	MNIST	98.59	98.52	98.51	98.56	98.62 (+)	98.53 (+)	98.51 (+)	98.56 (-)
	SVHN	88.58	88.96	89.20	88.75	89.90 (+)	89.02 (+)	89.22 (+)	89.91 (+)
	CIFAR-10	74.69	70.88	72.51	74.33	74.69 (+)	70.97 (+)	72.68 (+)	74.18 (-)
	CIFAR-100	71.78	71.65	71.96	71.95	72.06 (+)	71.91 (+)	72.19 (+)	72.24 (+)

In this section we verify the performance of our GT-DDP optimizer and discuss the benefit of having layer-wise feedback policies during weight update. Detail experiment setup and additional results are provided in the Appendix C.

We validate the performance of GT-DDP on digits recognition and image classification data set. The networks consist of 1-4 residual blocks followed by fully-connected (FC) layers (see Fig. 5), except that we use ResNet18 [21] for the CIFAR-100 dataset. Each block contains a skip connection between 3 convolution modules, possibly with a non-identity shortcut mapping if needed. Following the discussion in the previous section, we select our baselines as SGD, RMSprop [41], Adam [42], and EKFAC [31], as they cover most widely-used curvature approximation in training deep nets, including (adaptive) diagonal matrices and second-order Kronecker factorization.

Table 2 summarizes our main results. In each experiment we keep the shared hyper-parameters (e.g. learning rate and weight decay) between baselines and their GT-DDP variants the same, so that the performance difference only comes from GT-DDP framework. On all data set, GT-DDP achieves better or comparable results on both training and accuracy. Notably, when comparing original methods with their GT-DDP integrated variants, the latter improve training convergence on almost all dataset. Empirically, it also leads to better generalization.

Since the feedback updates are typically order of magnitude smaller than the open gain due to the sparse Hessian of standard classification loss (i.e. cross-entropy), GT-DDP follows similar training trend with the baseline it used to approximate the parameter curvature (see Fig. 6a). Nevertheless, these additional updates have a non-trivial effect on not only improving the convergence but robustifying the training. As shown in Fig. 6b, GT-DDP reduces the variation of the performance difference over random seeds subjected to same hyper-parameters⁶. In fact, the Bellman framework has been shown numerically stable than direct optimization such as Newton method [43], since it takes into account the temporal, i.e. layer-wise, structure inherit in Eq. (1). As the concern for reproducibility arises [44], GT-DDP provides a principled way to improve the robustness and consistency during training. We highlight this perspective as the benefit gained from *architecture-aware* optimization.

To understand the effect of feedback policies more perceptually, we conduct eigen-decomposition on the feedback matrices of convolution layers and project the leading eigenvectors back to image space, using techniques proposed in [45]. These feature maps, denoted δx_{\max} in Fig. 6c, correspond to the dominating differential image that GT-DDP policies shall respond with during weight update.

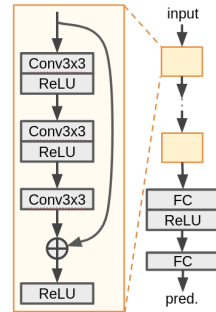


Figure 5: Architecture and residual block in Sec. 5.

⁶ Additional experiments across different hyper-parameters are provided in the Appendix C.

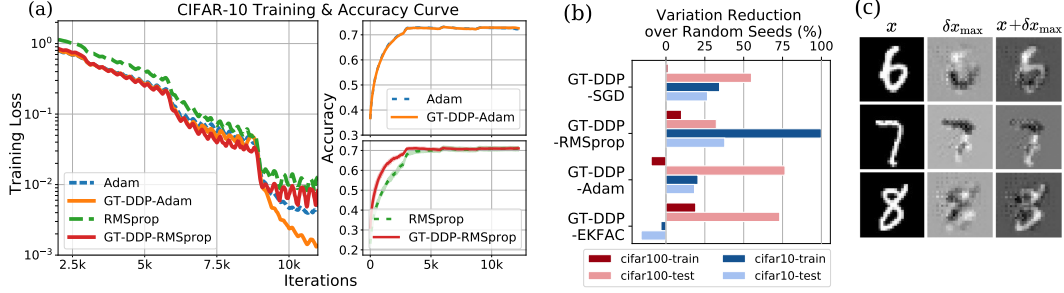


Figure 6: (a) Training performance on CIFAR-10 for Adam, RMSprop and their GT-DDP variants. (b) Variation reduction over 3-6 random seeds on CIFAR-10 and CIFAR-100. We report the value $(\text{VAR}_{\text{GT-DDP-Baseline}} - \text{VAR}_{\text{Baseline}}) / \text{VAR}_{\text{Baseline}}$. (c) Visualization of the feedback policies on MNIST.

Fig. 6c demonstrates that the feedback policies indeed capture non-trivial visual feature related to the pixel-wise difference between spatially similar classes, e.g. (8, 3) or (7, 1). We note that these differential maps differ from adversarial perturbation [46] as the former directly link the parameter update to the change in activation; thus being more interpretable.

6 Discussion on Game-Theoretic Second-order Optimizer

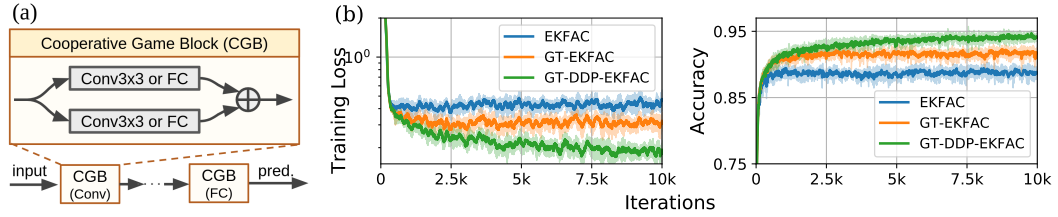


Figure 7: (a) Illustration of the cooperative-game module. (b) Training and testing performance on MNIST using the architecture in 7a. GT-EKFAC denotes integration of EKFAC with Corollary 7.

Theorem 3 may be of independent interest for developing game-theoretic second-order optimizer, as Eq.(16,17) provide efficient second-order approximation to the cooperative Hessian regardless of the presence of Bellman framework. To better show its effectiveness, let us consider the modules in Fig. 7a that resemble the cooperative game, i.e. two (p)layers take the same input and affect each payoff through output addition. Such an architecture has also appeared in recent work of progressive training [47]. Interestingly, for this particular structure, we have the following corollary to Thm. 3:

Corollary 7. Let $Q_{uu} \approx A_{uu} \otimes B_{uu} = U \Sigma_{uu} U^T$ be the eigen-decomposition of the Kronecker factorization, where $\Sigma_{uu} = \text{diag}(\lambda_{uu}) + \gamma I$ and $\gamma > 0$ is the Tikhonov damping. Consider the architecture in Fig. 7a, its cooperative matrix corresponds to rescaling in the eigenspace of Q_{uu} , i.e.

$$\tilde{Q}_{uu} = U \tilde{\Sigma}_{uu} U^T, \quad \tilde{\Sigma}_{uu} = \text{diag}(\tilde{\lambda}_{uu}) + \gamma I, \quad \text{and} \quad \tilde{\lambda}_{uu}^i = \frac{\gamma}{\gamma + \lambda_{uu}^i} \lambda_{uu}^i. \quad (24)$$

Notice that $\frac{\gamma}{\gamma + \lambda_{uu}^i} \leq 1$ for positive eigenvalues; thus the inverse Hessian \tilde{Q}_{uu}^{-1} shall take a larger step in eigenspace compared with Q_{uu}^{-1} . As shown in Fig 7b, integrating this game theoretic perspective with existing second-order methods, denoted GT-EKFAC, leads to better convergence. Having additional layer-wise policies from the GT-DDP framework further improves the performance.

7 Conclusion

In this work, we present the Game-Theoretic Differential Dynamic Programming (GT-DDP) optimizer as a new class of second-order algorithm. Theoretically, we strengthen the optimal control connection proposed in previous work by showing training residual networks can be linked to trajectory optimization in a cooperative game. Algorithmically, we propose several effective approximation which scales GT-DDP to training modern architectures and suggest how existing methods can be extended to accept such a game-theoretic perspective. We validate GT-DDP on several image classification dataset, showing improvement on both convergence and robustness.

Acknowledgments

The authors would like to thank Chen-Hsuan Lin, Yunpeng Pan, and Yen-Cheng Liu for many helpful discussions on the paper. The work is supported under Amazon AWS Machine Learning Research Award (MLRA).

References

- [1] Guan-Horng Liu, Tianrong Chen, and Evangelos A Theodorou. Differential dynamic programming neural optimizer. *arXiv preprint arXiv:2002.08809*, 2020.
- [2] Yiping Lu, Aoxiao Zhong, Quanzheng Li, and Bin Dong. Beyond finite layer neural networks: Bridging deep architectures and numerical differential equations. *arXiv preprint arXiv:1710.10121*, 2017.
- [3] Samuel S Schoenholz, Justin Gilmer, Surya Ganguli, and Jascha Sohl-Dickstein. Deep information propagation. *arXiv preprint arXiv:1611.01232*, 2016.
- [4] Ravid Shwartz-Ziv and Naftali Tishby. Opening the black box of deep neural networks via information. *arXiv preprint arXiv:1703.00810*, 2017.
- [5] Samuel Greydanus, Misko Dzamba, and Jason Yosinski. Hamiltonian neural networks. In *Advances in Neural Information Processing Systems*, pages 15353–15363, 2019.
- [6] Yaofeng Desmond Zhong, Biswadip Dey, and Amit Chakraborty. Symplectic ode-net: Learning hamiltonian dynamics with control. *arXiv preprint arXiv:1909.12077*, 2019.
- [7] E Weinan. A proposal on machine learning via dynamical systems. *Communications in Mathematics and Statistics*, 5(1):1–11, 2017.
- [8] Yiping Lu, Chao Ma, Yulong Lu, Jianfeng Lu, and Lexing Ying. A mean-field analysis of deep resnet and beyond: Towards provable optimization via overparameterization from depth. *arXiv preprint arXiv:2003.05508*, 2020.
- [9] Qi Sun, Yunzhe Tao, and Qiang Du. Stochastic training of residual networks: a differential equation viewpoint. *arXiv preprint arXiv:1812.00174*, 2018.
- [10] Bo Chang, Lili Meng, Eldad Haber, Lars Ruthotto, David Begert, and Elliot Holtham. Reversible architectures for arbitrarily deep residual neural networks. In *Thirty-Second AAAI Conference on Artificial Intelligence*, 2018.
- [11] Eldad Haber and Lars Ruthotto. Stable architectures for deep neural networks. *Inverse Problems*, 34(1):014004, 2017.
- [12] Tian Qi Chen, Yulia Rubanova, Jesse Bettencourt, and David K Duvenaud. Neural ordinary differential equations. In *Advances in Neural Information Processing Systems*, pages 6572–6583, 2018.
- [13] Xuanqing Liu, Tesi Xiao, Si Si, Qin Cao, Sanjiv Kumar, and Cho-Jui Hsieh. Neural ode: Stabilizing neural ode networks with stochastic noise. *arXiv preprint arXiv:1906.02355*, 2019.
- [14] Yuval Tassa, Tom Erez, and Emanuel Todorov. Synthesis and stabilization of complex behaviors through online trajectory optimization. In *2012 IEEE/RSJ International Conference on Intelligent Robots and Systems*, pages 4906–4913. IEEE, 2012.
- [15] E Weinan, Jiequn Han, and Qianxiao Li. A mean-field optimal control formulation of deep learning. *arXiv preprint arXiv:1807.01083*, 2018.
- [16] Guan-Horng Liu and Evangelos A Theodorou. Deep learning theory review: An optimal control and dynamical systems perspective. *arXiv preprint arXiv:1908.10920*, 2019.
- [17] Qianxiao Li and Shuji Hao. An optimal control approach to deep learning and applications to discrete-weight neural networks. *arXiv preprint arXiv:1803.01299*, 2018.
- [18] Qianxiao Li, Cheng Tai, and Weinan E. Stochastic modified equations and adaptive stochastic gradient algorithms. In *Proceedings of the 34th International Conference on Machine Learning-Volume 70*, pages 2101–2110. JMLR. org, 2017.
- [19] Dinghui Zhang, Tianyuan Zhang, Yiping Lu, Zhanxing Zhu, and Bin Dong. You only propagate once: Accelerating adversarial training via maximal principle. *arXiv preprint arXiv:1905.00877*, 2019.

- [20] Stefanie Gunther, Lars Ruthotto, Jacob B Schroder, Eric C Cyr, and Nicolas R Gauger. Layer-parallel training of deep residual neural networks. *SIAM Journal on Mathematics of Data Science*, 2(1):1–23, 2020.
- [21] Kaiming He, Xiangyu Zhang, Shaoqing Ren, and Jian Sun. Deep residual learning for image recognition. In *Proceedings of the IEEE conference on computer vision and pattern recognition*, pages 770–778, 2016.
- [22] Ian Goodfellow, Jean Pouget-Abadie, Mehdi Mirza, Bing Xu, David Warde-Farley, Sherjil Ozair, Aaron Courville, and Yoshua Bengio. Generative adversarial nets. In *Advances in neural information processing systems*, pages 2672–2680, 2014.
- [23] Naveen Kodali, Jacob Abernethy, James Hays, and Zsolt Kira. On convergence and stability of gans. *arXiv preprint arXiv:1705.07215*, 2017.
- [24] Lars Mescheder, Sebastian Nowozin, and Andreas Geiger. The numerics of gans. In *Advances in Neural Information Processing Systems*, pages 1825–1835, 2017.
- [25] David Balduzzi, Sebastien Racaniere, James Martens, Jakob Foerster, Karl Tuyls, and Thore Graepel. The mechanics of n-player differentiable games. *arXiv preprint arXiv:1802.05642*, 2018.
- [26] David Balduzzi. Grammars for games: a gradient-based, game-theoretic framework for optimization in deep learning. *Frontiers in Robotics and AI*, 2:39, 2016.
- [27] Amirata Ghorbani and James Zou. Neuron shapley: Discovering the responsible neurons. *arXiv preprint arXiv:2002.09815*, 2020.
- [28] Julian Stier, Gabriele Gianini, Michael Granitzer, and Konstantin Ziegler. Analysing neural network topologies: a game theoretic approach. *Procedia Computer Science*, 126:234–243, 2018.
- [29] James Martens and Roger Grosse. Optimizing neural networks with kronecker-factored approximate curvature. In *International conference on machine learning*, pages 2408–2417, 2015.
- [30] Roger Grosse and James Martens. A kronecker-factored approximate fisher matrix for convolution layers. In *International Conference on Machine Learning*, pages 573–582, 2016.
- [31] Thomas George, César Laurent, Xavier Bouthillier, Nicolas Ballas, and Pascal Vincent. Fast approximate natural gradient descent in a kronecker factored eigenbasis. In *Advances in Neural Information Processing Systems*, pages 9550–9560, 2018.
- [32] Richard Bellman. The theory of dynamic programming. Technical report, Rand corp santa monica ca, 1954.
- [33] David D Fan and Evangelos A Theodorou. Differential dynamic programming for time-delayed systems. In *2016 IEEE 55th Conference on Decision and Control (CDC)*, pages 573–579. IEEE, 2016.
- [34] Kaiming He, Xiangyu Zhang, Shaoqing Ren, and Jian Sun. Identity mappings in deep residual networks. In *European conference on computer vision*, pages 630–645. Springer, 2016.
- [35] David WK Yeung and Leon A Petrosjan. *Cooperative stochastic differential games*. Springer Science & Business Media, 2006.
- [36] Yunpeng Pan, Evangelos Theodorou, and Kaivalya Bakshi. Robust trajectory optimization: A cooperative stochastic game theoretic approach. In *Robotics: Science and Systems*, 2015.
- [37] Kamil Nar, Orhan Ocal, S Shankar Sastry, and Kannan Ramchandran. Cross-entropy loss and low-rank features have responsibility for adversarial examples. *arXiv preprint arXiv:1901.08360*, 2019.
- [38] José Lezama, Qiang Qiu, Pablo Musé, and Guillermo Sapiro. Ole: Orthogonal low-rank embedding-a plug and play geometric loss for deep learning. In *Proceedings of the IEEE Conference on Computer Vision and Pattern Recognition*, pages 8109–8118, 2018.
- [39] Vincent Dumoulin and Francesco Visin. A guide to convolution arithmetic for deep learning. *arXiv preprint arXiv:1603.07285*, 2016.
- [40] Matthew D Zeiler, Dilip Krishnan, Graham W Taylor, and Rob Fergus. Deconvolutional networks. In *2010 IEEE Computer Society Conference on computer vision and pattern recognition*, pages 2528–2535. IEEE, 2010.

- [41] Geoffrey Hinton, Nitish Srivastava, and Kevin Swersky. Neural networks for machine learning lecture 6a overview of mini-batch gradient descent. 2012.
- [42] Diederik P Kingma and Jimmy Ba. Adam: A method for stochastic optimization. *arXiv preprint arXiv:1412.6980*, 2014.
- [43] Li-zhi Liao and Christine A Shoemaker. Advantages of differential dynamic programming over newton’s method for discrete-time optimal control problems. Technical report, Cornell University, 1992.
- [44] Peter Henderson, Riashat Islam, Philip Bachman, Joelle Pineau, Doina Precup, and David Meger. Deep reinforcement learning that matters. In *Thirty-Second AAAI Conference on Artificial Intelligence*, 2018.
- [45] Matthew D Zeiler and Rob Fergus. Visualizing and understanding convolutional networks. In *European conference on computer vision*, pages 818–833. Springer, 2014.
- [46] Ian J Goodfellow, Jonathon Shlens, and Christian Szegedy. Explaining and harnessing adversarial examples. *arXiv preprint arXiv:1412.6572*, 2014.
- [47] Lemeng Wu, Dilin Wang, and Qiang Liu. Splitting steepest descent for growing neural architectures. In *Advances in Neural Information Processing Systems*, pages 10655–10665, 2019.
- [48] Gunter Stein. Respect the unstable. *IEEE Control systems magazine*, 23(4):12–25, 2003.
- [49] Emanuel Todorov and Weiwei Li. A generalized iterative lqg method for locally-optimal feedback control of constrained nonlinear stochastic systems. In *Proceedings of the 2005, American Control Conference, 2005.*, pages 300–306. IEEE, 2005.
- [50] Adam Paszke, Sam Gross, Soumith Chintala, Gregory Chanan, Edward Yang, Zachary DeVito, Zeming Lin, Alban Desmaison, Luca Antiga, and Adam Lerer. Automatic differentiation in pytorch. 2017.

Supplementary Material

A Derivation of Optimal Control Representation for Residual networks

A.1 Derivation in Section 3.1

First, recall the Bellman objective in feedforward networks, $Q_t(\mathbf{x}_t, \mathbf{u}_t) \triangleq \ell_t(\mathbf{u}_t) + V_{t+1}(f_t(\mathbf{x}_t, \mathbf{u}_t))$. Following standard chain rule, the second-order expansion of Q_t in Eq. (4) takes the form

$$\delta Q_t = \frac{1}{2} \begin{bmatrix} \mathbf{1} \\ \delta \mathbf{x}_t \\ \delta \mathbf{u}_t \end{bmatrix}^\top \begin{bmatrix} \mathbf{0} & Q_x^t & Q_u^t \\ Q_x^t & Q_{xx}^t & Q_{xu}^t \\ Q_u^t & Q_{ux}^t & Q_{uu}^t \end{bmatrix} \begin{bmatrix} \mathbf{1} \\ \delta \mathbf{x}_t \\ \delta \mathbf{u}_t \end{bmatrix}, \quad \begin{aligned} Q_x^t &= f_x^t \top V_x^{t+1} \\ Q_u^t &= f_u^t \top V_x^{t+1} + \ell_u^t \\ Q_{uu}^t &= f_u^t \top V_{xx}^{t+1} f_u^t + V_x^{t+1} \cdot f_{uu}^t + \ell_{uu}^t, \\ Q_{ux}^t &= f_u^t \top V_{xx}^{t+1} f_x^t + V_x^{t+1} \cdot f_{ux}^t \\ Q_{xx}^t &= f_x^t \top V_{xx}^{t+1} f_x^t + V_x^{t+1} \cdot f_{xx}^t \end{aligned} \quad (25)$$

where the dot notation represents the product of a vector with a 3D tensor. Note that in practice, the dynamics is often expanded up to the first order, i.e. by omitting $f_{xx}^t, f_{uu}^t, f_{ux}^t$ above, while keeping the full second-order expansion of the value function V_{xx}^{t+1} . This can be seen as Gauss-Newton (GN) approximation, and the stability obtained by keeping only the linearized dynamics is discussed thoroughly in trajectory optimization [14, 49]. As such, both DDP [1] and our GT-DDP optimizer adopt the same setup.

Now, let us consider the value minimization described in Eq. (8) for residual networks. We shall interpret the propagation rules as $\hat{f}_t(\hat{\mathbf{x}}_t, \mathbf{u}_t)$, where $\hat{\mathbf{x}}_t$ is the *residual-augmented* state $\hat{\mathbf{x}}_t \triangleq [\mathbf{x}_t, \mathbf{x}_r]^\top$. The Jacobian of this state-augmented dynamics and its relation to the ones in the absence of residual paths, i.e. f_x^t, f_u^t , can be summarized below:

$$\text{At } t = t_f, \text{ Eq. (8a) gives } \underbrace{\mathbf{x}_{t+1} = \mathbf{x}_r + f_t(\mathbf{x}_t, \mathbf{u}_t)}_{\hat{\mathbf{x}}_{t+1} = \hat{f}_t(\hat{\mathbf{x}}_t, \mathbf{u}_t)} \Rightarrow \hat{f}_{\hat{\mathbf{x}}}^t = \begin{bmatrix} f_x^t & \mathbf{I} \end{bmatrix}, \hat{f}_{\mathbf{u}}^t = f_u^t, \quad (26a)$$

$$\text{At } t \in (t_s, t_f), \text{ Eq. (8b) gives } \underbrace{\begin{bmatrix} \mathbf{x}_{t+1} \\ \mathbf{x}_r \end{bmatrix} = \begin{bmatrix} f_t(\mathbf{x}_t, \mathbf{u}_t) \\ \mathbf{x}_r \end{bmatrix}}_{\hat{\mathbf{x}}_{t+1} = \hat{f}_t(\hat{\mathbf{x}}_t, \mathbf{u}_t)} \Rightarrow \hat{f}_{\hat{\mathbf{x}}}^t = \begin{bmatrix} f_x^t & \mathbf{0} \\ \mathbf{0} & \mathbf{I} \end{bmatrix}, \hat{f}_{\mathbf{u}}^t = \begin{bmatrix} f_u^t \\ \mathbf{0} \end{bmatrix}, \quad (26b)$$

$$\text{At } t = t_s, \text{ Eq. (8c) gives } \underbrace{\begin{bmatrix} \mathbf{x}_{t+1} \\ \mathbf{x}_r \end{bmatrix} = \begin{bmatrix} f_t(\mathbf{x}_t, \mathbf{u}_t) \\ \mathbf{x}_t \end{bmatrix}}_{\hat{\mathbf{x}}_{t+1} = \hat{f}_t(\hat{\mathbf{x}}_t, \mathbf{u}_t)} \Rightarrow \hat{f}_{\hat{\mathbf{x}}}^t = \begin{bmatrix} f_x^t \\ \mathbf{I} \end{bmatrix}, \hat{f}_{\mathbf{u}}^t = \begin{bmatrix} f_u^t \\ \mathbf{0} \end{bmatrix}, \quad (26c)$$

where \mathbf{I} is the identity matrix.

Once we have the explicit form of dynamics written, the optimal control representation can be derived by substituting Eq. (26) into Eq. (25). After some algebra, one can verify that for $t \in (t_s, t_f]$ we will have

$$\hat{Q}_{\hat{\mathbf{x}}}^t = \hat{f}_{\hat{\mathbf{x}}}^t \top \hat{V}_{\hat{\mathbf{x}}}^{t+1} = [Q_x^t \quad V_{x_r}^{t+1}]^\top \quad (27a)$$

$$\hat{Q}_{\mathbf{u}}^t = \hat{f}_{\mathbf{u}}^t \top \hat{V}_{\hat{\mathbf{x}}}^{t+1} + \ell_u^t = Q_u^t \quad (27b)$$

$$\hat{Q}_{uu}^t = \hat{f}_{\mathbf{u}}^t \top \hat{V}_{\hat{\mathbf{x}}}^{t+1} \hat{f}_{\mathbf{u}}^t + \ell_{uu}^t = Q_{uu}^t \quad (27c)$$

$$\hat{Q}_{u\hat{\mathbf{x}}}^t = \hat{f}_{\mathbf{u}}^t \top \hat{V}_{\hat{\mathbf{x}}}^{t+1} \hat{f}_{\hat{\mathbf{x}}}^t = [Q_{ux}^t \quad f_u^t \top V_{x_r}^{t+1}] \quad (27d)$$

$$\hat{Q}_{\hat{\mathbf{x}}\hat{\mathbf{x}}}^t = \hat{f}_{\hat{\mathbf{x}}}^t \top \hat{V}_{\hat{\mathbf{x}}}^{t+1} \hat{f}_{\hat{\mathbf{x}}}^t = \begin{bmatrix} Q_{xx}^t & f_x^t \top V_{x_r}^{t+1} \\ V_{x_r, x}^{t+1} f_x^t & V_{x_r, x_r}^{t+1} \end{bmatrix}. \quad (27e)$$

The optimal feedback policy is given by

$$\delta \mathbf{u}_t^*(\delta \hat{\mathbf{x}}_t) = -(\hat{Q}_{uu}^t)^{-1} (\hat{Q}_{\mathbf{u}}^t + \hat{Q}_{u\hat{\mathbf{x}}}^t \delta \hat{\mathbf{x}}_t) = \mathbf{k}_t + \mathbf{K}_t \delta \mathbf{x}_t - \underbrace{(Q_{uu}^t)^{-1} f_u^t \top V_{x_r}^{t+1}}_{\triangleq \mathbf{G}_t} \delta \mathbf{x}_r, \quad (28)$$

Note that $\hat{V}_{\hat{\mathbf{x}}}^{t+1}$ and $\hat{V}_{\hat{\mathbf{x}}\hat{\mathbf{x}}}^{t+1}$ are the derivatives of the value function $\hat{V}_{t+1}(\hat{\mathbf{x}}_{t+1})$ induced by the state-augmented dynamics. We can compute these matrices backward from t_f similar to Eq. (6):

$$\hat{V}_{\hat{\mathbf{x}}}^t = \hat{Q}_{\hat{\mathbf{x}}}^t - \hat{Q}_{\hat{\mathbf{x}}\mathbf{u}}^t (\hat{Q}_{\mathbf{u}\mathbf{u}}^t)^{-1} \hat{Q}_{\mathbf{u}}^t = \begin{bmatrix} Q_{\mathbf{x}}^t + Q_{\mathbf{x}\mathbf{u}}^t \mathbf{k}_t \\ V_{\mathbf{x}_r}^{t+1} - \mathbf{G}_t^\top Q_{\mathbf{u}\mathbf{u}}^t \mathbf{k}_t \end{bmatrix} \triangleq \begin{bmatrix} V_{\mathbf{x}}^t \\ V_{\mathbf{x}_r}^t \end{bmatrix}, \quad (29)$$

$$\begin{aligned} \hat{V}_{\hat{\mathbf{x}}\hat{\mathbf{x}}}^t &= \hat{Q}_{\hat{\mathbf{x}}\hat{\mathbf{x}}}^t - \hat{Q}_{\hat{\mathbf{x}}\mathbf{u}}^t (\hat{Q}_{\mathbf{u}\mathbf{u}}^t)^{-1} \hat{Q}_{\mathbf{u}\hat{\mathbf{x}}}^t = \begin{bmatrix} Q_{\mathbf{x}\mathbf{x}}^t + Q_{\mathbf{x}\mathbf{u}}^t \mathbf{K}_t & f_{\mathbf{x}}^{t\top} V_{\mathbf{x}\mathbf{x}_r}^{t+1} - \mathbf{K}_t^\top Q_{\mathbf{u}\mathbf{u}}^t \mathbf{G}_t \\ V_{\mathbf{x}_r\mathbf{x}}^{t+1} f_{\mathbf{x}}^t - \mathbf{G}_t^\top Q_{\mathbf{u}\mathbf{u}}^t \mathbf{K}_t & V_{\mathbf{x}_r\mathbf{x}_r}^{t+1} - \mathbf{G}_t^\top Q_{\mathbf{u}\mathbf{u}}^t \mathbf{G}_t \end{bmatrix} \\ &\triangleq \begin{bmatrix} V_{\mathbf{x}\mathbf{x}}^t & V_{\mathbf{x}\mathbf{x}_r}^t \\ V_{\mathbf{x}_r\mathbf{x}}^t & V_{\mathbf{x}_r\mathbf{x}_r}^t \end{bmatrix}, \end{aligned} \quad (30)$$

with the terminal conditions given by $V_{\mathbf{x}_r}^{t_f+1} = V_{\mathbf{x}}^{t_f+1}$ and $V_{\mathbf{x}_r\mathbf{x}_r}^{t_f+1} = V_{\mathbf{x}\mathbf{x}_r}^{t_f+1} = V_{\mathbf{x}_r\mathbf{x}}^{t_f+1} = V_{\mathbf{x}\mathbf{x}}^{t_f+1}$.

As for the stage $t = t_s$ where the residual state is split out, the derivatives of Q_t follow (again one can readily verify by substituting Eq. (26c) into Eq. (25)) by

$$\hat{Q}_{\hat{\mathbf{x}}}^{t_s} = Q_{\mathbf{x}}^{t_s} + V_{\mathbf{x}_r}^{t_s+1}, \quad (31a)$$

$$\hat{Q}_{\mathbf{u}\hat{\mathbf{x}}}^{t_s} = Q_{\mathbf{u}\mathbf{x}}^{t_s} + f_{\mathbf{u}}^{t_s\top} V_{\mathbf{x}\mathbf{x}_r}^{t_s+1}, \quad (31b)$$

$$\hat{Q}_{\hat{\mathbf{x}}\hat{\mathbf{x}}}^{t_s} = Q_{\mathbf{x}\mathbf{x}}^{t_s} + f_{\mathbf{x}}^{t_s\top} V_{\mathbf{x}\mathbf{x}_r}^{t_s+1} + V_{\mathbf{x}_r\mathbf{x}}^{t_s+1} f_{\mathbf{x}}^t + V_{\mathbf{x}_r\mathbf{x}_r}^{t_s+1}, \quad (31c)$$

and $\hat{Q}_{\mathbf{u}}^t$ and $\hat{Q}_{\mathbf{u}\mathbf{u}}^t$ remain the same with $Q_{\mathbf{u}}^t$ and $Q_{\mathbf{u}\mathbf{u}}^t$. The resulting optimal policy admits the same form as in Eq. (28).

Proof of Proposition 2: Finally, one can verify Eq. (11, 12) by noticing that the derivatives of the value function at $t = t_s$ follow

$$\begin{aligned} \tilde{V}_{\mathbf{x}}^{t_s} &= \hat{Q}_{\hat{\mathbf{x}}}^{t_s} - \hat{Q}_{\hat{\mathbf{x}}\mathbf{u}}^{t_s} (\hat{Q}_{\mathbf{u}\mathbf{u}}^{t_s})^{-1} \hat{Q}_{\mathbf{u}}^{t_s} \\ &= (Q_{\mathbf{x}}^{t_s} + Q_{\mathbf{x}\mathbf{u}}^{t_s} \mathbf{k}_{t_s}) + (V_{\mathbf{x}_r}^{t_s+1} - f_{\mathbf{u}}^{t_s\top} V_{\mathbf{x}\mathbf{x}_r}^{t_s+1} \mathbf{k}_{t_s}) \\ &= V_{\mathbf{x}}^{t_s} + V_{\mathbf{x}_r}^{t_s+1} - \mathbf{G}_{t_s}^\top Q_{\mathbf{u}\mathbf{u}}^{t_s} \mathbf{k}_{t_s} \\ &= V_{\mathbf{x}}^{t_s} + V_{\mathbf{x}}^{t_f+1} - \sum_{t \in [t_s, t_f]} \mathbf{G}_t^\top Q_{\mathbf{u}\mathbf{u}}^t \mathbf{k}_t, \end{aligned} \quad (32)$$

$$\begin{aligned} \tilde{V}_{\mathbf{x}\mathbf{x}}^{t_s} &= \hat{Q}_{\hat{\mathbf{x}}\hat{\mathbf{x}}}^{t_s} - \hat{Q}_{\hat{\mathbf{x}}\mathbf{u}}^{t_s} (\hat{Q}_{\mathbf{u}\mathbf{u}}^{t_s})^{-1} \hat{Q}_{\mathbf{u}\hat{\mathbf{x}}}^{t_s} \\ &= (Q_{\mathbf{x}\mathbf{x}}^{t_s} + Q_{\mathbf{x}\mathbf{u}}^{t_s} \mathbf{K}_{t_s}) + (f_{\mathbf{x}}^{t_s\top} V_{\mathbf{x}\mathbf{x}_r}^{t_s+1} - \mathbf{K}_{t_s}^\top Q_{\mathbf{u}\mathbf{u}}^{t_s} \mathbf{G}_{t_s}) \\ &\quad + (V_{\mathbf{x}_r\mathbf{x}}^{t_s+1} f_{\mathbf{x}}^t - \mathbf{G}_{t_s}^\top Q_{\mathbf{u}\mathbf{u}}^{t_s} \mathbf{K}_{t_s}) + (V_{\mathbf{x}_r\mathbf{x}_r}^{t_s+1} - \mathbf{G}_{t_s}^\top Q_{\mathbf{u}\mathbf{u}}^{t_s} \mathbf{G}_{t_s}) \\ &= V_{\mathbf{x}\mathbf{x}}^{t_s} + V_{\mathbf{x}\mathbf{x}_r}^{t_s} + V_{\mathbf{x}\mathbf{x}_r}^{t_s\top} + V_{\mathbf{x}_r\mathbf{x}_r}^{t_s+1} - \mathbf{G}_{t_s}^\top Q_{\mathbf{u}\mathbf{u}}^{t_s} \mathbf{G}_{t_s} \\ &= V_{\mathbf{x}\mathbf{x}}^{t_s} + V_{\mathbf{x}\mathbf{x}_r}^{t_s} + V_{\mathbf{x}\mathbf{x}_r}^{t_s\top} + V_{\mathbf{x}\mathbf{x}}^{t_f+1} - \sum_{t \in [t_s, t_f]} \mathbf{G}_t^\top Q_{\mathbf{u}\mathbf{u}}^t \mathbf{G}_t, \end{aligned} \quad (33)$$

where the last equalities in Eq. (32, 33) follow by applying the recursions

$$\begin{aligned} V_{\mathbf{x}_r}^t &\triangleq V_{\mathbf{x}_r}^{t+1} - \mathbf{G}_t^\top Q_{\mathbf{u}\mathbf{u}}^t \mathbf{k}_t, & V_{\mathbf{x}_r}^{t_f+1} &= V_{\mathbf{x}}^{t_f+1} \\ V_{\mathbf{x}_r\mathbf{x}_r}^t &\triangleq V_{\mathbf{x}_r\mathbf{x}_r}^{t+1} - \mathbf{G}_t^\top Q_{\mathbf{u}\mathbf{u}}^t \mathbf{G}_t, & V_{\mathbf{x}_r\mathbf{x}_r}^{t_f+1} &= V_{\mathbf{x}\mathbf{x}}^{t_f+1}. \end{aligned} \quad (34)$$

Thus we conclude the proof.

A.2 Derivation in Section 3.2

Here we provide the derivation of Eq. (14, 15). Recall in Eq. (13) the cooperative Bellman objective $Q_t(\mathbf{x}_r, \mathbf{x}_t, \mathbf{u}_t, \mathbf{v}_t)$ and expand it wrt all variables to the second order.

$$\delta Q_t = \frac{1}{2} \begin{bmatrix} \mathbf{1} \\ \delta \mathbf{x}_t \\ \delta \mathbf{x}_r \\ \delta \mathbf{u}_t \\ \delta \mathbf{v}_t \end{bmatrix}^\top \begin{bmatrix} \mathbf{0} & Q_{\mathbf{x}}^t & Q_{\mathbf{x}_r}^t & Q_{\mathbf{u}}^t & Q_{\mathbf{v}}^t \\ Q_{\mathbf{x}}^t & Q_{\mathbf{x}\mathbf{x}}^t & Q_{\mathbf{x}\mathbf{x}_r}^t & Q_{\mathbf{x}\mathbf{u}}^t & Q_{\mathbf{x}\mathbf{v}}^t \\ Q_{\mathbf{x}_r}^t & Q_{\mathbf{x}_r\mathbf{x}}^t & Q_{\mathbf{x}_r\mathbf{x}_r}^t & Q_{\mathbf{x}_r\mathbf{u}}^t & Q_{\mathbf{x}_r\mathbf{v}}^t \\ Q_{\mathbf{u}}^t & Q_{\mathbf{u}\mathbf{x}}^t & Q_{\mathbf{u}\mathbf{x}_r}^t & Q_{\mathbf{u}\mathbf{u}}^t & Q_{\mathbf{u}\mathbf{v}}^t \\ Q_{\mathbf{v}}^t & Q_{\mathbf{v}\mathbf{x}}^t & Q_{\mathbf{v}\mathbf{x}_r}^t & Q_{\mathbf{v}\mathbf{u}}^t & Q_{\mathbf{v}\mathbf{v}}^t \end{bmatrix} \begin{bmatrix} \mathbf{1} \\ \delta \mathbf{x}_t \\ \delta \mathbf{x}_r \\ \delta \mathbf{u}_t \\ \delta \mathbf{v}_t \end{bmatrix}. \quad (35)$$

Similar to section A.1 where we consider the augmented state $\hat{\mathbf{x}}_t \triangleq [\mathbf{x}_t, \mathbf{x}_r]^\top$, here we can additionally interpret the joint control as $\hat{\mathbf{u}}_t \triangleq [\mathbf{u}_t, \mathbf{v}_t]^\top$. The derivatives of the state-control-augmented Bellman objective $\hat{Q}_t(\hat{\mathbf{x}}_r, \hat{\mathbf{u}}_t)$ thus follow

$$\hat{Q}_{\hat{\mathbf{u}}}^t = \begin{bmatrix} Q_{\mathbf{u}}^t \\ Q_{\mathbf{v}}^t \end{bmatrix}, \quad \hat{Q}_{\hat{\mathbf{u}}\hat{\mathbf{x}}}^t = \begin{bmatrix} Q_{\mathbf{u}\mathbf{x}}^t & Q_{\mathbf{u}\mathbf{x}_r}^t \\ Q_{\mathbf{v}\mathbf{x}}^t & Q_{\mathbf{v}\mathbf{x}_r}^t \end{bmatrix}, \quad \hat{Q}_{\hat{\mathbf{u}}\hat{\mathbf{u}}}^t = \begin{bmatrix} Q_{\mathbf{u}\mathbf{u}}^t & Q_{\mathbf{u}\mathbf{v}}^t \\ Q_{\mathbf{v}\mathbf{u}}^t & Q_{\mathbf{v}\mathbf{v}}^t \end{bmatrix}, \quad (36)$$

and the feedback policy in this case is given by

$$\begin{aligned} \delta \hat{\mathbf{u}}_t^*(\delta \hat{\mathbf{x}}_t) &= -(\hat{Q}_{\hat{\mathbf{u}}\hat{\mathbf{u}}}^t)^{-1}(\hat{Q}_{\hat{\mathbf{u}}}^t + \hat{Q}_{\hat{\mathbf{u}}\hat{\mathbf{x}}}^t \delta \hat{\mathbf{x}}_t) \\ &= -\begin{bmatrix} Q_{\mathbf{u}\mathbf{u}}^t & Q_{\mathbf{u}\mathbf{v}}^t \\ Q_{\mathbf{v}\mathbf{u}}^t & Q_{\mathbf{v}\mathbf{v}}^t \end{bmatrix}^{-1} \left(\begin{bmatrix} Q_{\mathbf{u}}^t \\ Q_{\mathbf{v}}^t \end{bmatrix} + \begin{bmatrix} Q_{\mathbf{u}\mathbf{x}}^t & Q_{\mathbf{u}\mathbf{x}_r}^t \\ Q_{\mathbf{v}\mathbf{x}}^t & Q_{\mathbf{v}\mathbf{x}_r}^t \end{bmatrix} \delta \hat{\mathbf{x}}_t \right). \end{aligned} \quad (37)$$

Now, we apply the block-matrices inversion with the Schur complement by recalling

$$\begin{bmatrix} Q_{\mathbf{u}\mathbf{u}}^t & Q_{\mathbf{u}\mathbf{v}}^t \\ Q_{\mathbf{v}\mathbf{u}}^t & Q_{\mathbf{v}\mathbf{v}}^t \end{bmatrix}^{-1} = \begin{bmatrix} \overbrace{(Q_{\mathbf{u}\mathbf{u}}^t - Q_{\mathbf{u}\mathbf{v}}^t(Q_{\mathbf{v}\mathbf{v}}^t)^{-1}Q_{\mathbf{v}\mathbf{u}}^t)^{-1}}^{\tilde{Q}_{\mathbf{u}\mathbf{u}}^t} & -(\tilde{Q}_{\mathbf{u}\mathbf{u}}^t)^{-1}Q_{\mathbf{u}\mathbf{v}}^t(Q_{\mathbf{v}\mathbf{v}}^t)^{-1} \\ -(\tilde{Q}_{\mathbf{v}\mathbf{v}}^t)^{-1}Q_{\mathbf{v}\mathbf{u}}^t(Q_{\mathbf{u}\mathbf{u}}^t)^{-1} & \underbrace{(Q_{\mathbf{v}\mathbf{v}}^t - Q_{\mathbf{v}\mathbf{u}}^t(Q_{\mathbf{u}\mathbf{u}}^t)^{-1}Q_{\mathbf{u}\mathbf{v}}^t)^{-1}}_{\tilde{Q}_{\mathbf{v}\mathbf{v}}^t} \end{bmatrix}. \quad (38)$$

Substitute Eq. (38) into Eq. (37) and after some algebra, we will arrive at

$$\delta \hat{\mathbf{u}}_t^*(\delta \hat{\mathbf{x}}_t) = \begin{bmatrix} \tilde{\mathbf{K}}_t \\ \tilde{\mathbf{I}}_t \end{bmatrix} + \begin{bmatrix} \tilde{\mathbf{K}}_t & \tilde{\mathbf{G}}_t \\ \tilde{\mathbf{H}}_t & \tilde{\mathbf{L}}_t \end{bmatrix} \delta \hat{\mathbf{x}}_t = \begin{bmatrix} \tilde{\mathbf{K}}_t + \tilde{\mathbf{K}}_t \delta \mathbf{x}_t + \tilde{\mathbf{G}}_t \delta \mathbf{x}_r \\ \tilde{\mathbf{I}}_t + \tilde{\mathbf{H}}_t \delta \mathbf{x}_t + \tilde{\mathbf{L}}_t \delta \mathbf{x}_r \end{bmatrix} \triangleq \begin{bmatrix} \delta \mathbf{u}_t^*(\delta \mathbf{x}_t, \delta \mathbf{x}_r) \\ \delta \mathbf{v}_t^*(\delta \mathbf{x}_t, \delta \mathbf{x}_r) \end{bmatrix}, \quad (39)$$

where

$$\tilde{\mathbf{K}}_t = -(\tilde{Q}_{\mathbf{u}\mathbf{u}}^t)^{-1}(Q_{\mathbf{u}}^t - Q_{\mathbf{u}\mathbf{v}}^t(Q_{\mathbf{v}\mathbf{v}}^t)^{-1}Q_{\mathbf{v}}^t), \quad (40a)$$

$$\tilde{\mathbf{K}}_t = -(\tilde{Q}_{\mathbf{u}\mathbf{u}}^t)^{-1}(Q_{\mathbf{u}\mathbf{x}}^t - Q_{\mathbf{u}\mathbf{v}}^t(Q_{\mathbf{v}\mathbf{v}}^t)^{-1}Q_{\mathbf{v}\mathbf{x}}^t), \quad (40b)$$

$$\tilde{\mathbf{G}}_t = -(\tilde{Q}_{\mathbf{u}\mathbf{u}}^t)^{-1}(Q_{\mathbf{u}\mathbf{x}_r}^t - Q_{\mathbf{u}\mathbf{v}}^t(Q_{\mathbf{v}\mathbf{v}}^t)^{-1}Q_{\mathbf{v}\mathbf{x}_r}^t), \quad (40c)$$

$$\tilde{\mathbf{I}}_t = -(\tilde{Q}_{\mathbf{v}\mathbf{v}}^t)^{-1}(Q_{\mathbf{v}}^t - Q_{\mathbf{v}\mathbf{u}}^t(Q_{\mathbf{u}\mathbf{u}}^t)^{-1}Q_{\mathbf{u}}^t), \quad (40d)$$

$$\tilde{\mathbf{H}}_t = -(\tilde{Q}_{\mathbf{v}\mathbf{v}}^t)^{-1}(Q_{\mathbf{v}\mathbf{x}}^t - Q_{\mathbf{v}\mathbf{u}}^t(Q_{\mathbf{u}\mathbf{u}}^t)^{-1}Q_{\mathbf{u}\mathbf{x}}^t), \quad (40e)$$

$$\tilde{\mathbf{L}}_t = -(\tilde{Q}_{\mathbf{v}\mathbf{v}}^t)^{-1}(Q_{\mathbf{v}\mathbf{x}_r}^t - Q_{\mathbf{v}\mathbf{u}}^t(Q_{\mathbf{u}\mathbf{u}}^t)^{-1}Q_{\mathbf{u}\mathbf{x}_r}^t), \quad (40f)$$

which conclude Eq. (14, 15).

B Derivation in Section 4

B.1 Preliminary on Second-Order Kronecker Factorization

Popular curvature factorization methods, such as KFAC [29] and EKFac [31], rely on the fact that for feedforward networks:

$$\mathbf{x}_{t+1} = \sigma_t(\mathbf{h}_t), \quad \mathbf{h}_t \equiv \mathbf{W}_t \mathbf{x}_t + \mathbf{b}_t, \quad (41)$$

where σ_t is the nonlinear activation function and \mathbf{h}_t denotes the pre-activation vector, we have $J_{\mathbf{u}}^t = \mathbf{x}_t \otimes J_{\mathbf{h}}^t$. \otimes denotes the Kronecker product and J_t is the per-stage objective defined in Eq. (3). Thus, the Gauss-Newton (GN) approximation of $J_{\mathbf{u}\mathbf{u}}^t$ can be computed as

$$J_{\mathbf{u}\mathbf{u}}^t \approx \mathbb{E}[J_{\mathbf{u}}^t J_{\mathbf{u}}^{t\top}] = \mathbb{E}[(\mathbf{x}_t \otimes J_{\mathbf{h}}^t)(\mathbf{x}_t \otimes J_{\mathbf{h}}^t)^\top] \approx \mathbb{E}[(\mathbf{x}_t \mathbf{x}_t^\top)] \otimes \mathbb{E}[(J_{\mathbf{h}}^t J_{\mathbf{h}}^{t\top})], \quad (42)$$

where the expectation is taken over the mini-batch.

The factorization in Eq. (42) is also applicable to DDP and GT-DDP, as Eq. (41) can be expressed by $\mathbf{x}_{t+1} = f_t(\mathbf{x}_t, \mathbf{u}_t)$, with $\mathbf{u}_t \triangleq [\text{vec}(\mathbf{W}_t), \mathbf{b}_t]^\top$; thus it is a valid dynamics. Further, we have

$$f_{\mathbf{u}}^{t\top} V_x^{t+1} = \mathbf{x}_t \otimes V_{\mathbf{h}}^t, \quad \text{where } V_{\mathbf{h}}^t = \sigma_{\mathbf{h}}^{t\top} V_x^{t+1} \quad (43)$$

is the derivative of the value function wrt to the pre-activation. Following similar derivation, we will arrive at the Kronecker approximation of Q_{uu}^t :

$$Q_{uu}^t \approx \mathbb{E}[Q_u^t Q_u^{t\top}] = \mathbb{E}[(\mathbf{x}_t \otimes V_h^t)(\mathbf{x}_t \otimes V_h^t)^\top] \approx \mathbb{E}[\mathbf{x}_t \mathbf{x}_t^\top] \otimes \mathbb{E}[V_h^t V_h^{t\top}]. \quad (44)$$

The Kronecker factorization allows us to compute the preconditioned update efficiently by noticing that for matrices $\mathbf{A} \in \mathbb{R}^{n \times n}$, $\mathbf{B} \in \mathbb{R}^{m \times m}$, and $\mathbf{X} \in \mathbb{R}^{m \times n}$, we have

$$(\mathbf{A} \otimes \mathbf{B}) \text{vec}(\mathbf{X}) = \text{vec}(\mathbf{B} \mathbf{X} \mathbf{A}^\top), \quad (45)$$

where vec denotes the vectorization. Here, we shall interpret \mathbf{A} and \mathbf{B} respectively as $\mathbb{E}[\mathbf{x}_t \mathbf{x}_t^\top]$ and $\mathbb{E}[V_h^t V_h^{t\top}]$. Additionally, the following properties will become handy for the later derivation.

$$(\mathbf{A} \otimes \mathbf{B})^{-1} = \mathbf{A}^{-1} \otimes \mathbf{B}^{-1} \quad (46)$$

$$(\mathbf{A} \otimes \mathbf{B})^\top = \mathbf{A}^\top \otimes \mathbf{B}^\top. \quad (47)$$

B.2 Derivation of Theorem 3

Let us consider two distinct layers, $f(\mathbf{x}_u, \mathbf{u})$ and $h(\mathbf{x}_v, \mathbf{v})$, and denote the propagation rules of their pre-activation, along with the Kronecker factorization, respectively as

$$\begin{aligned} \mathbf{h}_u &= \mathbf{u} \mathbf{x}_u, & Q_{uu} &\approx \mathbb{E}[\mathbf{x}_u \mathbf{x}_u^\top] \otimes \mathbb{E}[\mathbf{g}_u \mathbf{g}_u^\top] \triangleq A_{uu} \otimes B_{uu}, \\ \mathbf{h}_v &= \mathbf{v} \mathbf{x}_v, & Q_{vv} &\approx \mathbb{E}[\mathbf{x}_v \mathbf{x}_v^\top] \otimes \mathbb{E}[\mathbf{g}_v \mathbf{g}_v^\top] \triangleq A_{vv} \otimes B_{vv}, \end{aligned} \quad (48)$$

where $\mathbf{g}_u \equiv V_{h_u}$ and $\mathbf{g}_v \equiv V_{h_v}$ for notational simplicity. We drop the bias in the propagation rules but note that our derivation extends to the bias cases. Following Eq. (45, 46), the preconditioned update, take \mathbf{k}_t for instance, can be computed by $\mathbf{k}_t \triangleq -Q_{uu}^{-1} \text{vec}(Q_u) \approx -\text{vec}(B_{uu}^{-1} Q_u A_{uu}^{-\top})$.

Now consider the CG formulation where the two layers are placed parallel in a residual network. A.2 suggests that one can derive the cooperative representation by considering the joint parametrization $[\mathbf{u}, \mathbf{v}]^\top$ and state augmentation $\hat{\mathbf{x}} = [\mathbf{x}_u, \mathbf{x}_v]^\top$. To this end, we interpret Eq. (48) as an augmented dynamics and rewrite it compactly as

$$\begin{bmatrix} \mathbf{h}_u \\ \mathbf{h}_v \end{bmatrix} = \begin{bmatrix} \mathbf{u} & \mathbf{0} \\ \mathbf{0} & \mathbf{v} \end{bmatrix} \begin{bmatrix} \mathbf{x}_u \\ \mathbf{x}_v \end{bmatrix} \Leftrightarrow \hat{\mathbf{h}} = \mathbf{w} \hat{\mathbf{x}}. \quad (49)$$

The approximated Hessian can thus be factorized as $Q_{ww} \approx A_{ww} \otimes B_{ww}$, where

$$\begin{aligned} A_{ww} &= \mathbb{E}[\hat{\mathbf{x}} \hat{\mathbf{x}}^\top] = \begin{bmatrix} \mathbb{E}[\mathbf{x}_u \mathbf{x}_u^\top] & \mathbb{E}[\mathbf{x}_u \mathbf{x}_v^\top] \\ \mathbb{E}[\mathbf{x}_v \mathbf{x}_u^\top] & \mathbb{E}[\mathbf{x}_v \mathbf{x}_v^\top] \end{bmatrix} = \begin{bmatrix} A_{uu} & A_{uv} \\ A_{vu} & A_{vv} \end{bmatrix} \\ B_{ww} &= \mathbb{E}[\hat{\mathbf{g}} \hat{\mathbf{g}}^\top] = \begin{bmatrix} \mathbb{E}[\mathbf{g}_u \mathbf{g}_u^\top] & \mathbb{E}[\mathbf{g}_u \mathbf{g}_v^\top] \\ \mathbb{E}[\mathbf{g}_v \mathbf{g}_u^\top] & \mathbb{E}[\mathbf{g}_v \mathbf{g}_v^\top] \end{bmatrix} = \begin{bmatrix} B_{uu} & B_{uv} \\ B_{vu} & B_{vv} \end{bmatrix} \end{aligned} \quad (50)$$

are the Kronecker blocks. Their inverse matrices are given by the Schur component (c.f. Eq. (38)):

$$\begin{aligned} A_{ww}^{-1} &= \begin{bmatrix} \tilde{A}_{uu}^{-1} & -\tilde{A}_{uu}^{-1} A_{uv} A_{vv}^{-1} \\ -\tilde{A}_{vv}^{-1} A_{vu} A_{uu}^{-1} & \tilde{A}_{vv}^{-1} \end{bmatrix}, & \text{where } \begin{cases} \tilde{A}_{uu} \triangleq A_{uu} - A_{uv} A_{vv}^{-1} A_{vu} \\ \tilde{A}_{vv} \triangleq A_{vv} - A_{uv} A_{vv}^{-1} A_{vu} \end{cases} \\ B_{ww}^{-1} &= \begin{bmatrix} \tilde{B}_{uu}^{-1} & -\tilde{B}_{uu}^{-1} B_{uv} B_{vv}^{-1} \\ -\tilde{B}_{vv}^{-1} B_{vu} B_{uu}^{-1} & \tilde{B}_{vv}^{-1} \end{bmatrix}, & \text{where } \begin{cases} \tilde{B}_{uu} \triangleq B_{uu} - B_{uv} B_{vv}^{-1} B_{vu} \\ \tilde{B}_{vv} \triangleq B_{vv} - B_{uv} B_{vv}^{-1} B_{vu} \end{cases} \end{aligned} \quad (51)$$

Now, we are ready to derive Theorem 3. First notice that the preconditioned open gain can be computed by

$$-Q_{ww}^{-1} \text{vec} \left(\begin{bmatrix} Q_u & \mathbf{0} \\ \mathbf{0} & Q_v \end{bmatrix} \right) = -(A_{ww}^{-1} \otimes B_{ww}^{-1}) \text{vec} \left(\begin{bmatrix} Q_u & \mathbf{0} \\ \mathbf{0} & Q_v \end{bmatrix} \right) = -\text{vec}(B_{ww}^{-1} \begin{bmatrix} Q_u & \mathbf{0} \\ \mathbf{0} & Q_v \end{bmatrix} A_{ww}^{-\top}) \quad (52)$$

Expanding Eq. (52) by substituting B_{ww}^{-1} and $A_{ww}^{-\top}$ with Eq. (51), after some algebra we will arrive at

$$\begin{aligned} \tilde{\mathbf{k}} &\approx -\text{vec}(\tilde{B}_{uu}^{-1} Q_u \tilde{A}_{uu}^{-\top} + \tilde{B}_{uu}^{-1} B_{uv} B_{vv}^{-1} Q_v (\tilde{A}_{uu}^{-1} A_{uv} A_{vv}^{-1})^\top), \\ \tilde{\mathbf{l}} &\approx -\text{vec}(\tilde{B}_{vv}^{-1} Q_v \tilde{A}_{vv}^{-\top} + \tilde{B}_{vv}^{-1} B_{vu} B_{uu}^{-1} Q_u (\tilde{A}_{vv}^{-1} A_{vu} A_{uu}^{-1})^\top), \end{aligned} \quad (53)$$

which give the *Kronecker approximation of the cooperative open gains*. The Kronecker factorization for each cooperative matrix can be obtained by decomposed Eq. (53) into the following

$$\begin{aligned}
\tilde{\mathbf{k}} &= -\text{vec}(\tilde{B}_{uu}^{-1}Q_u\tilde{A}_{uu}^{-\top} + \tilde{B}_{uu}^{-1}B_{uv}B_{vv}^{-1}Q_v(\tilde{A}_{uu}^{-1}A_{uv}A_{vv}^{-1})^\top) \\
&= -\text{vec}(\tilde{B}_{uu}^{-1}(Q_u + B_{uv}B_{vv}^{-1}Q_vA_{vv}^{-\top}A_{uv}^\top)\tilde{A}_{uu}^{-\top}) \\
&= -(\tilde{A}_{uu}^{-1} \otimes \tilde{B}_{uu}^{-1})\text{vec}(Q_u + B_{uv}B_{vv}^{-1}Q_vA_{vv}^{-\top}A_{uv}^\top) \\
&= -(\tilde{A}_{uu}^{-1} \otimes \tilde{B}_{uu}^{-1})(\text{vec}(Q_u) + \text{vec}(B_{uv}B_{vv}^{-1}Q_vA_{vv}^{-\top}A_{uv}^\top)) \\
&= -(\tilde{A}_{uu}^{-1} \otimes \tilde{B}_{uu}^{-1})(\text{vec}(Q_u) + (A_{uv} \otimes B_{uv})\text{vec}(B_{vv}^{-1}Q_vA_{vv}^{-\top})) \\
&= -\underbrace{(\tilde{A}_{uu}^{-1} \otimes \tilde{B}_{uu}^{-1})}_{\approx \tilde{Q}_{uu}^{-1}}(\text{vec}(Q_u) + \underbrace{(A_{uv} \otimes B_{uv})}_{\approx -Q_{uv}}\underbrace{(A_{vv}^{-1} \otimes B_{vv}^{-1})}_{\approx Q_{vv}^{-1}}\text{vec}(Q_v)),
\end{aligned} \tag{54}$$

where we recall the definition $\tilde{\mathbf{k}} \triangleq -\tilde{Q}_{uu}^{-1}(\text{vec}(Q_u) - Q_{uv}Q_{vv}^{-1}\text{vec}(Q_v))$. Similarly, it can be readily verified that $\tilde{Q}_{vv}^{-1} \approx \tilde{A}_{vv}^{-1} \otimes \tilde{B}_{vv}^{-1}$. Note that when Q_{uv} vanishes, i.e. $A_{uv} = B_{uv} = \mathbf{0}$, Eq. (54) will degenerate to original Kronecker factorization for the non-cooperative update. Thus, we conclude the proof.

B.3 Derivation of Corollary 7

Before deriving Corollary 7, we first review the eigen-basis representation of the Kronecker approximation appeared in George et al. [31]. Recall the factorization $Q_{uu} \approx A_{uu} \otimes B_{uu}$ and let $A_{uu} = U_A \Sigma_A U_A^\top$, $B_{uu} = U_B \Sigma_B U_B^\top$ be their eigen-decomposition. We can rewrite the Kronecker factorization in its eigen-basis

$$\begin{aligned}
A_{uu} \otimes B_{uu} &= (U_A \Sigma_A U_A^\top) \otimes (U_B \Sigma_B U_B^\top) \\
&= (U_A \otimes U_B)(\Sigma_A \otimes \Sigma_B)(U_A \otimes U_B)^\top \\
&\triangleq U \Sigma_{uu} U^\top,
\end{aligned} \tag{55}$$

where U is the eigen-basis of the Kronecker factorization. $\Sigma_{uu} \triangleq \text{diag}(\lambda_{uu})$ contains eigenvalues along the diagonal entries. In practice, we will also add a positive Tikhonov coefficient $\gamma > 0$ for regularization purpose.

Now, observe that for the cooperative game module in Fig. 7a, we have

$$A_{uu} = A_{uv} = A_{vv}, \quad B_{uu} = B_{uv} = B_{vv}, \tag{56}$$

since the two layers share the same input $\mathbf{x}_u = \mathbf{x}_v$ and output derivative $\mathbf{g}_u = \mathbf{g}_v$. In other words, Q_{uv} and Q_{vv} are factorized by the same Kronecker blocks with Q_{uu} ; thus they share the same eigen-basis U . The cooperative matrix \tilde{Q}_{uu} can thus be rewritten as

$$\begin{aligned}
\tilde{Q}_{uu} &= Q_{uu} - Q_{uv}Q_{vv}^{-1}Q_{uv}^\top \\
&= A_{uu} \otimes B_{uu} - (-A_{uv} \otimes B_{uv})(A_{vv} \otimes B_{vv})^{-1}(-A_{uv} \otimes B_{uv})^\top \\
&= U(\gamma \mathbf{I} + \Sigma_{uu})U^\top - (-U \Sigma_{uu} U^\top)(U(\gamma \mathbf{I} + \Sigma_{uu})^{-1}U^\top)(-U \Sigma_{uu} U^\top)^\top \\
&= U \tilde{\Sigma}_{uu} U^\top,
\end{aligned} \tag{57}$$

where $\tilde{\Sigma}_{uu} = \gamma \mathbf{I} + \text{diag}(\tilde{\lambda}_{uu})$ and

$$\tilde{\lambda}_{uu}^i = \lambda_{uu}^i - \frac{(\lambda_{uu}^i)^2}{\gamma + \lambda_{uu}^i} = \frac{\gamma}{\gamma + \lambda_{uu}^i} \lambda_{uu}^i. \tag{58}$$

In short, the cooperative matrix \tilde{Q}_{uu} admits a scaling in the eigen-basis of its non-cooperative variant.

B.4 Proof for Proposition 4

Recall the connection we made in Sec. 2.1 and 2.2. It is sufficient to show that when the two conditions in Proposition 4 are met, we will have Eq. (4, 5) collapse exactly with Eq. (2, 3). First, notice that at the final layer, we have $V_x^\top = J_x^\top = \nabla_x \phi$ and $V_{xx}^\top = J_{xx}^\top = \nabla_x^2 \phi$ without any condition. Further, Eq. (29, 30) suggest that when all mixed partial derivatives between parameter and

activation vanish, the backward dynamics of (V_x^t, V_{xx}^t) degenerates to (Q_x^t, Q_{xx}^t) . The derivatives of J_t wrt x_t in this case (c.f. Eq. (3)),

$$J_x^t = f_x^{t\top} J_x^{t+1}, \quad J_{xx}^t = f_x^{t\top} J_{xx}^{t+1} f_x^t,$$

are the same as the backward dynamics for (V_x^t, V_{xx}^t) ,

$$V_x^t = Q_x^t = f_x^{t\top} V_x^{t+1}, \quad V_{xx}^t = Q_{xx}^t = f_x^{t\top} V_{xx}^{t+1} f_x^t.$$

Thus the two functionals J_t and V_t coincide with each other.

Next, when the parameters between distinct layers are uncorrelated, we will have $Q_{uv}^t = Q_{vu}^t = 0$ at all stages. The cooperative precondition matrices, if exist along the network, degenerate to the curvature approximation it uses to approximate the parameter Hessian. In fact, we will have

$$Q_u^t = J_u^t, \quad \tilde{Q}_{uu}^t = Q_{uu}^t = J_{uu}^t.$$

Thus, the update rule Eq. (4) also collapses to Eq. (2).

C Experiment Detail

C.1 Experiment Setup in Section 5 and 6

Network architectures for classification task are shown in Fig. 5. We use 1 residual block for DIGITS, MNIST, SVHN dataset and 4 residual blocks for CIFAR-10. For CIFAR-100, we use ResNet18 [21] architecture. All networks use ReLU activation for the intermediate layers and identity mapping at the last prediction layer. The batch size is set to 128 for all data set except 8 for DIGITS. As for section 6, the network contains 3 convolution CGBs (c.f. Fig. 7a), 1 fully-connected CGB, and finally 1 standard fully-connected layer with identity mapping. We use Tanh activation for this experiment but note that similar trend can be observed for ReLU. The batch size is set to 12. Regarding the machine information, we conduct our experiments on GTX 1080 TI, RTX TITAN, four Tesla V100 SXM2 16GB on AWS, and eight GTX TITAN X. All experiments are implemented and conducted with Pytorch [50]. We use the implementation in <https://github.com/Thrandis/EKFAC-pytorch> for EKFAC baseline.

C.2 Additional Result and Discussion

Variation Reduction Over Different Learning Rate. Recall Fig. 6b reports the variation reduction on the hyper-parameter used in Table 2. Here we provide additional results and show that the robustness gained from GT-DDP integration remains consistent across different hyper-parameters. Particularly, in Fig. 8 we report the variance difference on 3 different learning rates for each GT-DDP variant. We use the same setup as in Fig. 5, i.e. we keep all hyper-parameters the same for each experiment so that the performance difference only comes from the existence of feedback policies. For all cases, having additional updates from GT-DDP stabilizes the training dynamics by reducing its variation over random initialization.

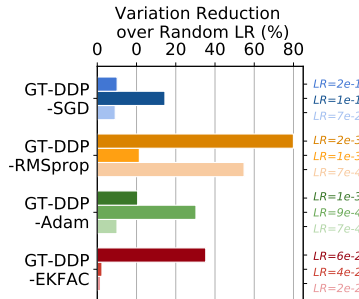


Figure 8: Variation reduction over 3 different learning rates for each GT-DDP variant on CIFAR-10. We report the value $(\text{VAR}_{\text{GT-DDP-Baseline}} - \text{VAR}_{\text{Baseline}}) / \text{VAR}_{\text{Baseline}}$, where each variance is computed over 3 random seeds.